Bioorganic Chemistry 110 (2021) 104801

Contents lists available at ScienceDirect

Bioorganic Chemistry

journal homepage: www.elsevier.com/locate/bioorg

Discovery of novel tetrahydrobenzo[*b*]thiophene-3-carbonitriles as histone deacetylase inhibitors

Piyush Gediya [a], Vivek K. Vyas [a], Vincenzo Carafa [b], Nikum Sitwala [a], Laura Della Torre [b], Angelita Poziello [b], Takashi Kurohara [c], Takayoshi Suzuki [c], Vinod Sanna [d], Varalakshmi Raguraman [e], K. Suthindhiran [e], Debarpan Ghosh [f], Dhiraj Bhatia [f], Lucia Altucci [b,*], Manjunath D. Ghate [a,*]

[a] *Department of Pharmaceutical Chemistry, Institute of Pharmacy, Nirma University, Ahmedabad 382481, Gujarat, India*
[b] *Department of Precision Medicine, Università degli Studi della Campania "Luigi Vanvitelli", Via L. De Crecchio 7, 80138 Naples, Italy*
[c] *The Institute of Scientific and Industrial Research (ISIR), Osaka University, Mihogaoka, Ibarakishi, Osaka 567-0047, Japan*
[d] *Piramal Pharma Solution, Plot-18 Pharmaceutical Special Economic Zone, Sarkhej-Bawla, NH-8A, Ahmedabad, Gujarat 382213, India*
[e] *School of Bio-Sciences and Technology, Vellore Institute of Technology, Vellore, Tamilnadu, India*
[f] *Department of Biological Engineering, Indian Institute of Technology, Gandhinagar 382355, Gujarat, India*

ARTICLE INFO

Keywords:
HDAC inhibitors
Anticancer agents
Cyclic linkers
Benzo[*b*]thiophene-3-carbonitriles

ABSTRACT

The discovery and development of isoform-selective histone deacetylase (HDAC) inhibitor is a challenging task because of the sequence homology among HDAC enzymes. In the present work, novel tetrahydro benzo[*b*] thiophene-3-carbonitrile based benzamides were designed, synthesized, and evaluated as HDAC inhibitors. Pharmacophore modeling was our main design strategy, and two novel series of tetrahydro benzo[*b*]thiophene-3-carbonitrile derivatives with piperidine linker (series 1) and piperazine linker (series 2) were identified as HDAC inhibitors. Among all the synthesised compounds, **9h** with 4-(aminomethyl) piperidine linker and **14n** with piperazine linker demonstrated good activity against human HDAC1 and HDAC6, respectively. Both the compounds also exhibited good antiproliferative activity against several human cancer cell lines. Both these compounds (**9h** and **14n**) also induced cell cycle arrest and apoptosis in U937 and MDA-MB-231 cancer cells. Overall, for the first time, this research discovered potent isoform-selective HDAC inhibitors using cyclic linker instead of the aliphatic chain and aromatic ring system, which were reported in known HDAC inhibitors.

1. Introduction

Histone deacetylases (HDACs) regulate the expression of many proteins, which are studied intensively over the past few years. HDACs are epigenetically regulated and overexpression play crucial roles in several biological processes, whose alteration led to the development of many diseases including cancer [1–3]. Many small molecules are known as HDAC inhibitors, and they demonstrated significant effects against various types of cancer (Fig. 1) [4]. Histone is a core part of HDAC enzyme, which plays an important role in epigenetic regulation [5] via alteration of different chemical reactions i.e. acetylation, deacetylation, and methylation. Acetylation of histone increases transcription and deacetylation leads to inhibition of transcription. Inhibition of transcription causes deregulation of enzyme functions, which leads to various abrupt effects on the cell cycle. Disruption in the progression of the cell cycle causes various types of cancer as well as other diseases. Inhibition of HDACs leads to an increased level of acetylated histone, bringing about a variety of dependent cell events like apoptosis, cell differentiation, cell survival, and inhibition of cell proliferation [6]. In recent decades, HDACs have emerged as potential targets for the treatment of cancer and neurodegenerative diseases [7]. HDAC enzymes are classified into four different classes based on phylogenetic properties: class I (HDAC1, 2, 3 and 8), class II (class IIa: HDAC4, 5, 7, 9; and class IIb: HDAC6, 10), class III (sirtuins SIRT1-7), and class IV (HDAC11). HDAC classes I, II, and IV are zinc-dependent enzymes and class III HDACs are NAD^+ dependent enzymes. Chemical structures of known

Abbreviations: HDAC, Histone deacetylase; DCM, Dichloromethane; TEA, Triethylamine; TFA, Trifluoroacetic acid; TLC, thin-layer chromatography; PI, propidium iodide.

* Corresponding authors.
E-mail addresses: lucia.altucci@unicampania.it (L. Altucci), manjunath.ghate@nirmauni.ac.in (M.D. Ghate).

https://doi.org/10.1016/j.bioorg.2021.104801
Received 2 January 2021; Received in revised form 27 February 2021; Accepted 1 March 2021
Available online 5 March 2021

HDAC inhibitors are comprised of three-components: 1) cap region for surface recognition; 2) a linker, and; 3) a zinc-binding group (ZBG) [8]. HDAC inhibitors have an electron donor group in their structures, which is mainly involved in the zinc-binding due to its ability to chelate active site zinc ions [9]. HDAC1, 2 and 3 inhibitors are considered as the key targets for the development of anticancer agents. To treat cutaneous T cell lymphoma (CTCL) and multiple myeloma, USFDA approved few HDAC inhibitors such as vorinostat (SAHA®) [10], panobinostat (LBH-589) [11] and belinostat (PXD-101) [12] (Fig. 1). In the year 2015, panobinostat, a pan-HDAC inhibitor was approved for the treatment of multiple myeloma.

Many other HDAC inhibitors are in clinical trials, either as a single drug or in combination with other agents to treat solid tumors and hematological cancers, such as pracinostat (SB939) [13], entinostat (MS275) [14], and rocilinostat (ACY-1215) [15] (Fig. 1). However, most of the approved HDAC inhibitors are pan-HDAC or class I inhibitors. Due to the lack of selectivity or partial selectivity of these inhibitors, some undesirable responses such as cardiotoxicity was observed. Also, clinically approved HDAC inhibitors are less effective against solid tumors. Thus, an increasing number of studies concentrate on the discovery and development of isoform-selective HDAC inhibitors to prevent/reduce adverse effects and achieve efficacy against solid tumors.

With this aim, herein we described the discovery of novel tetrahydrobenzo[*b*]thiophene-3-carbonitriles as selective HDAC1 and HDAC6 inhibitors as anticancer agents. Our laboratory is mainly involved in the search of novel anticancer agents [16–18], which are acting on known biological anticancer targets. Herein, we would like to present novel HDAC inhibitors as potent anticancer agents.

2. Results and discussion

2.1. Rational design using pharmacophore modeling

The known pharmacophore model of HDAC inhibitors consist of a cap group, a linker, and a zinc-binding group (ZBG) [19]. Cap moiety mainly interacts with the important amino acid residues present at the surface of an enzyme that recognizes the HDAC isoform. A hydrophobic carbon chain linker joins the cap with ZBG and a zinc-binding group (ZBG) chelates Zn^{2+} ion at the catalytic domain [20]. To design novel HDAC inhibitors, we performed pharmacophore modeling with the known HDAC inhibitors (Fig. S1. under Electronic Supplementary Information). Generated pharmacophore models were validated using receiver operating characteristic (ROC) analysis and Günere-Henry (GH) scoring method. The best pharmacophore model suggested the presence of the four features (one acceptor atom, one donor atom, and two hydrophobic sites) for the design of novel HDAC inhibitors. For the design of the inhibitors, we selected a heterocyclic ring system as a core structure and functional groups as suggested by the generated pharmacophore model. We have also taken the reported pharmacophore (cap, linker and ZBG) into the consideration. As suggested by the pharmacophore model, for the first hydrophobic site, which was recognized as the cap group in the molecules, we selected 2-amino-4,5,6,7-tetrahydrobenzo[*b*]thiophene-3-carbonitrile ring. 2-Amino-4,5,6,7-tetrahydrobenzo[*b*]thiophene-3-carbonitrile ring also serves the purpose of the cap region in the molecules [8]. For one acceptor and one donor atoms identified in generated pharmacophore model, we selected an amide linker. This also serves the purpose of connecting unit (CU) as per the reported HDAC inhibitors pharmacophore model. Piperazine and piperidin-4-yl methanamine rings were selected as the second hydrophobic sites, which are recognized as hydrophobic linkers as per the

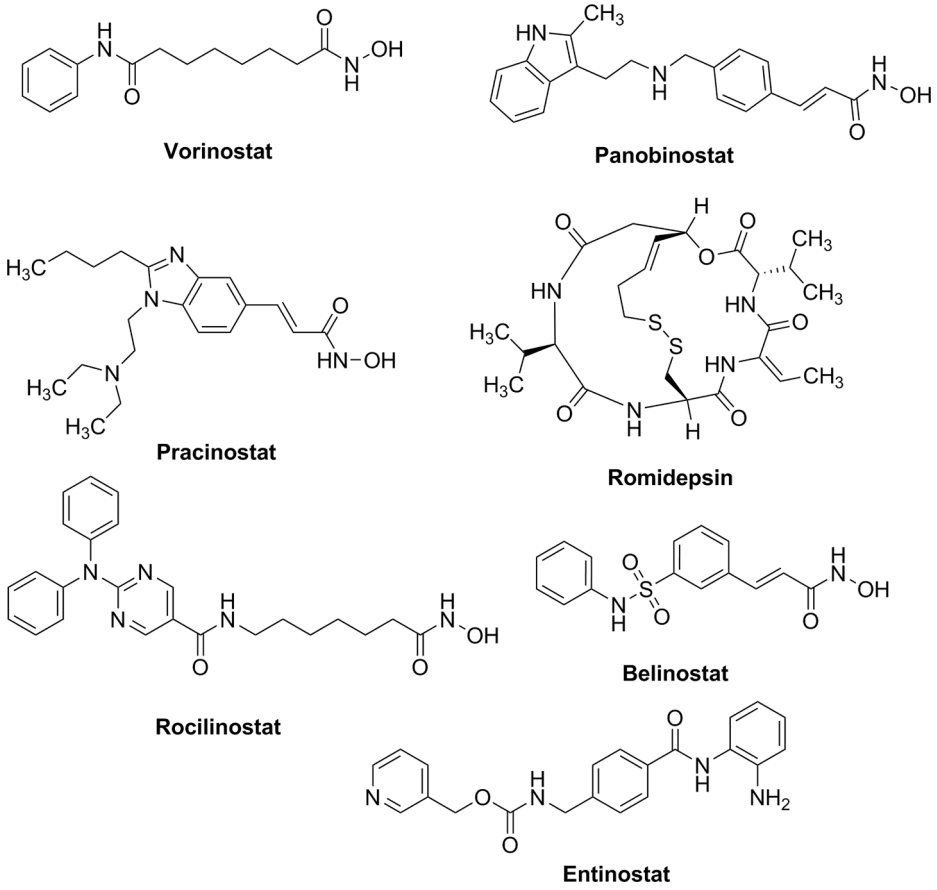

Fig. 1. Chemical structures of known HDAC inhibitors.

reported model. Various groups such as methyl, methoxy, halogen, and amine were introduced as ZBG in the designed molecules. The overall design strategy is depicted in Fig. 2.

2.2. Chemistry

A wide variety of synthetic routes were investigated and after analyses of all possible variations including the use of specific reaction conditions, catalysts, temperature range, reagents, etc., target compounds of both the series were synthesized. The general method for the synthesis of target compounds (**9a-o**) of series 1 with piperidine linker is illustrated in Scheme 1. Step 1 involves the Gewald reaction, in which a tetrahydro benzo[*b*]thiophene-3-carbonitrile ring was synthesized. This reaction was carried out in-between readily available cyclohexanone (**1**) as a starting material and malononitrile (**2**), in presence of sulphur (S_8) and morpholine as a base in absolute ethanol to afford first intermediate 2-amino-4,5,6,7-tetrahydrobenzo[*b*]thiophene-3-carbonitrile (**3**). In the next step, **3** was reacted with chloro acetyl chloride in the presence of dioxane to obtain 2-chloro-*N*-(3-cyano-4,5,6,7-tetrahydrobenzo[*b*]thiophen-2-yl)acetamide (**4**). This is a typical amide bond formation reaction using highly reactive acid chloride without any base. After removal of unreacted acyl chloride through filtration, buff-colored pure intermediate **4** was obtained. In another reaction, commercially available mono BOC (*tert*-butyloxycarbonyl) protected aliphatic cyclic diamine (*tert*-butyl 4-(aminomethyl)piperidine-1-carboxylate (**5**) was reacted with substituted acid chlorides and sulphonyl chlorides (**6a-o**) to form amide and sulfonamide bonds, and to obtain compounds **7a-o** in the presence of base triethylamine (TEA) and dichloromethane (DCM). The crude intermediates **7a-o** were dried in rotavapor and suspended in diethyl ether to get pure compounds **7a-o**. To further derivatize, BOC

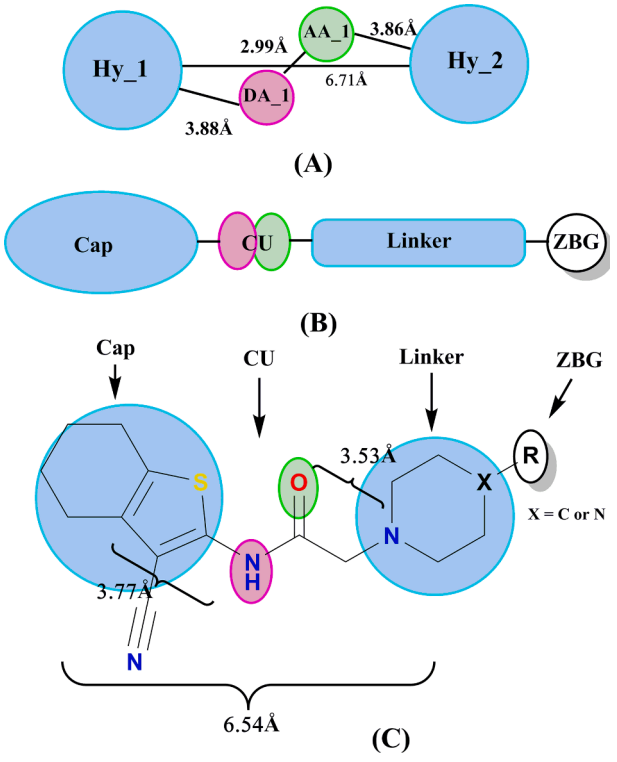

Fig. 2. Design strategy for the design of tetrahydrobenzo[*b*]thiophene-3-carbonitrile using pharmacophore modelling. (A) Generated two-dimensional pharmacophore hypothesis: AA_1 is acceptor atom; DA_1 is donor atom; and HY_1 and HY_2 are hydrophobic sites (B) Known pharmacophore model of HDAC inhibitors. (C) Design of tetrahydrobenzo[*b*]thiophene-3-carbonitrile derivatives as per the generated pharmacophore model (A) and correlated with reported pharmacophore model (B) with distance measured in Å.

protection was removed using typical acidic condition with trifluoroacetic acid (TFA) in DCM, which resulted in TFA salt of intermediates **8a-o**. The crude intermediates **8a-o** were suspended in diethyl ether to yield pure compounds **8a-o**. In the final step of Scheme 1, these intermediates (**8a-o**) were reacted with **4** in presence of base TEA in dioxane (halogen amine coupling) at 60 °C. An excess amount of TEA was used to neutralize TFA at elevated temperature, which afforded final target compounds **9a-o** of series 1. In Scheme 2, one of the compound **9g** of series 1 with a nitro group was reduced in the presence of Zn, NH_4Cl to yield compound **10** with a free amine group. Purification of intermediates and final compounds was carried out using column chromatography. The final compounds of series 1 were characterized using Mass, NMR, and FT-IR spectroscopy. Synthesized compounds (**9a-o**) of series 1 showed characteristic peaks of carbonyl (C═O) stretching around 1600–1500 cm^{-1}, nitrile (C—N) stretching peaks near 2210–2200 cm^{-1}, aromatic C—H stretching peaks near 3045–3010 cm^{-1}, aliphatic C—H stretching peaks near 2970–2930 cm^{-1} and amide bond stretching peaks near 3400–3200 cm^{-1} in FT-IR spectra. All the molecules showed M+H stable base peak in the mass analysis (**Electronic Supplementary Information**). Significant features of all compounds were observed in ^{1}H NMR spectra. Amide protons of the fused ring appeared in a range of 6.4 to 8.5 (δ) ppm as a singlet peak based on the surrounding environment. Protons of the aromatic ring system were observed as multiplet in a range of 6.7–8.0 (δ) ppm. For para substitution on the aromatic ring system, we observed doublet of doublet (dd) in the aromatic regions for all the compounds. The aromatic amide protons were observed as a broad peak near 10.5 (δ) ppm (**Electronic Supplementary Information**). Similarly, in ^{13}C NMR spectra, the peaks of an amide carbon atom attached to the aromatic system were observed at 167 (δ) ppm, and carbon atom attached to the aliphatic system was appeared at 166 ppm for all the compounds along with sets of aromatic carbon atoms, which were observed in the range of 120–140 (δ) ppm. Furthermore, the carbon atoms of the cyclic aliphatic ring were observed in the range of 20–60 (δ) ppm for all the synthesized compounds of series 1 (**Electronic Supplementary Information**).

To understand the structure–activity relationship (SAR) of linkers, we synthesized series 2 compounds with piperazine linker group with decreased chain length as depicted in Scheme 3. Alternatively, free aliphatic halogen of intermediate **4** was reacted with mono-BOC protected piperazine (**11**) through halogen amine coupling reaction using strong base K_2CO_3 at elevated temperature to afford intermediate **12**. BOC protection was removed using typical acidic conditions with trifluoroacetic acid (TFA), which resulted in TFA salt as crude intermediate **13**. Compound **13** was evaporated to dryness and suspended in diethyl ether to give pure intermediate **13**. The key intermediate **13** was reacted with **6a-o** (different substituted aliphatic/aromatic acid chlorides and sulphonyl chlorides) in presence of excess amount of TEA to neutralize TFA and to obtain the final target compounds of series 2 (**14a-o**). Compound **14g** was reduced using Zn and NH_4Cl to obtain compound **15** with a free amine group (Scheme 4). The final compounds of series 2 were characterized using Mass, NMR, and FT-IR. Purification of intermediates and final compounds was carried out using column chromatography. Series 2 molecules (**14a–o**), indicated characteristic peaks of acidic carbonyl (C═O) stretching around 1700–1550 cm^{-1}, nitrile (C—N) stretching peaks around 2210–2200 cm^{-1}, aromatic C—H stretching peaks near 3050–2950 cm^{-1}, aliphatic C—H stretching peaks near 2850–2650 cm^{-1} and amide stretching peaks near 3500–3300 cm^{-1} in FT-IR spectra. In the mass spectrum, all the molecules demonstrated a stable base peak as M+H (**Electronic Supplementary Information**). Significant features of all the synthesized compounds were observed in ^{1}H NMR spectra. A peak of amide proton was appeared in a range of 10.30–10.40 (δ) ppm as singlet based on the surrounding environment, along with aromatic protons mostly observed as a multiplet at 6.7–8.0 (δ) ppm. For, para substitution on the aromatic system, we observed doublet of doublet (dd) in the aromatic regions for all the compounds. In ^{13}C NMR spectra, the peaks of amide carbon attached to

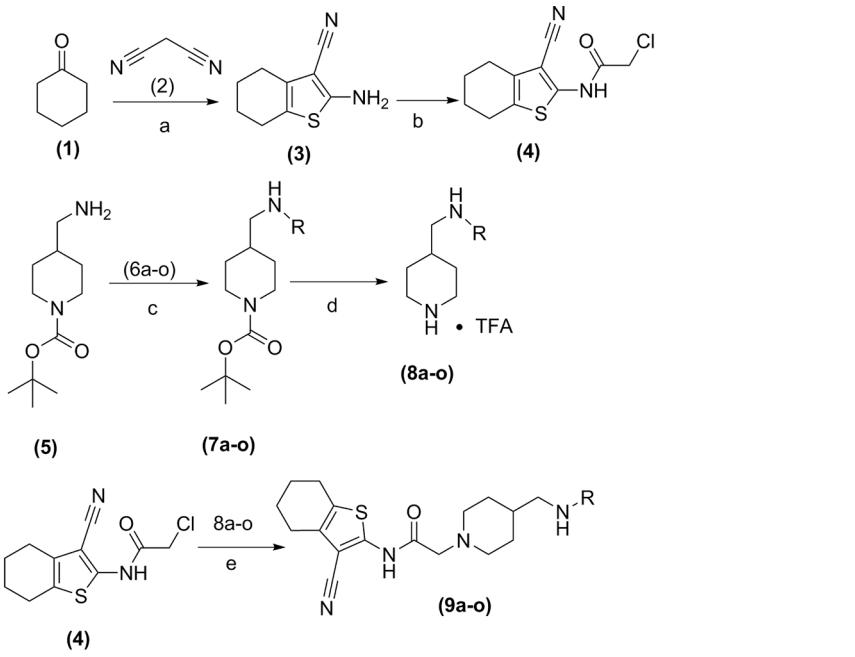

6a = 4-Methylbenzoyl chloride; **6b** = 4-Methoxybenzoyl chloride; **6c** = Benzoyl chloride; **6d** = 4-Chlorobenzoyl chloride; **6e** = 4-Bromobenzoyl chloride; **6f** = Ethyl chlorooxoacetate; **6g** = 4-Nitrobenzoyl chloride; **6h** = Acetyl chloride; **6i** = Benzenesulfonyl chloride; **6j** = 4-Methylbenzylsulfonyl chloride; **6k** = 4-Methoxybenzenesulfonyl chloride; **6l** = 4-Chlorobenzenesulfonyl chloride; **6m** = 2-Thiophenesulfonyl Chloride; **6n** = Methanesulfonyl chloride; **6o** = 4-Fluorobenzenesulfonyl chloride

Scheme 1. Synthetic scheme for the synthesis of 2-(4-(aminomethyl)piperidin-1-yl)-*N*-(3-cyano-4,5,6,7-tetrahydrobenzo[*b*]thiophen-2-yl)acetamide derivatives (**9a-o**). **Reagents and condition:** (a) sulphur S_8, morpholine, ethanol, 0–5 °C to rt, 1 h (b) chloro acetyl chloride, dioxane, rt, 30 min (c) TEA, DCM, rt, 30 min (d) TFA, DCM, rt, 30 min to 4 h. (e) TEA, dioxane, 60 °C.

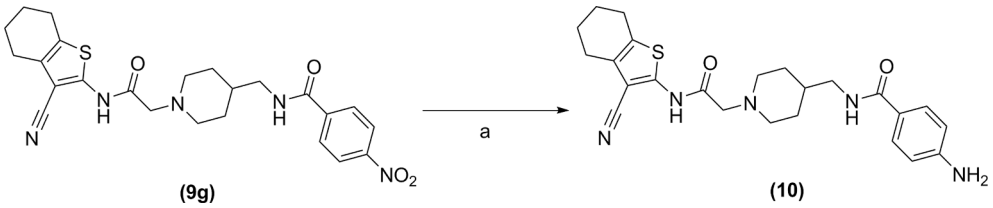

Scheme 2. Synthetic scheme for the synthesis of 4-amino-*N*-((1-(2-((3-cyano-4,5,6,7-tetrahydrobenzo[*b*]thiophen-2-yl)amino)-2-oxoethyl)piperidin-4-yl)methyl) benzamide (**10**). **Reagents and condition:** (a) Zn, NH_4Cl, water, methanol, 45 °C, 3 h.

the aromatic system were observed at 170–171 (δ) ppm and carbon atoms attached to the aliphatic system appeared at 166–167 (δ) ppm. Carbon atoms of the cyclic aliphatic ring were observed in the range of 21–61(δ) ppm for all the synthesized molecules along with sets of aromatic carbons observed from 126 to 146 (δ) pm (**Electronic Supplementary Information**). The purity of the final compounds of both the series was assessed by high-performance liquid chromatography (HPLC) and all the final compounds have >95% purity (**Electronic Supplementary Information**).

2.3. Biology

2.3.1. In vitro inhibition of HeLa cell nuclear broth

We initiated the screening of all the synthesized compounds of both the series against Hela cell nuclear broth as it is a rich source of HDAC1 and HDAC2 at a concentration of 10 μM. The inhibitory data is presented in Table S1 and S2 under Electronic Supplementary Information. Selected compounds with the highest inhibition were tested at different concentrations and IC_{50} values were determined (Table 1). Structure-activity relationship (SAR) studies of series 1 compounds (piperidin-4-ylmethanamine linker) with amide and sulphonamide groups as ZBG was explored here. Compound **9h** consisted of methyl amide, was one of the most potent compound with an IC_{50} value of 1.7 μM. Compound **10** with a 4-NH_2 group (reduction of 4–NO_2 of **9g**) and **9o** with 4-F group were also found active with IC_{50} values of 2.9 and 2.8 μM, respectively. To study the role of linkers, we synthesized series 2 with a piperazine aliphatic ring system, which is one carbon short than piperidin-4-ylmethanamine analogs. In series 2 compounds, a less crowded sulfonamides group with —CH_3 substitution in **14i** was observed with an IC_{50} value of 2.8 μM against HeLa cell nuclear broth. Similarly, compound **15** with 4-NH_2 had an IC_{50} value of 3.2 μM. Standard vorinostat was observed with an IC_{50} value of 3.3 μM. These results indicated that an aliphatic —CH_3 group attached with amide and sulphonamide ZBG, instead of an aromatic ring is important for better activity.

2.3.2. In vitro HDAC isoform selectivity

HDAC isoforms selective activity was performed against HDAC1, HDAC2, HDAC4, and HDAC6 enzymes at 10 μM concentration for the selected synthesized compounds (Table S3 under Electronic Supplementary Information). HDAC1 and HDAC2 are the member of class I

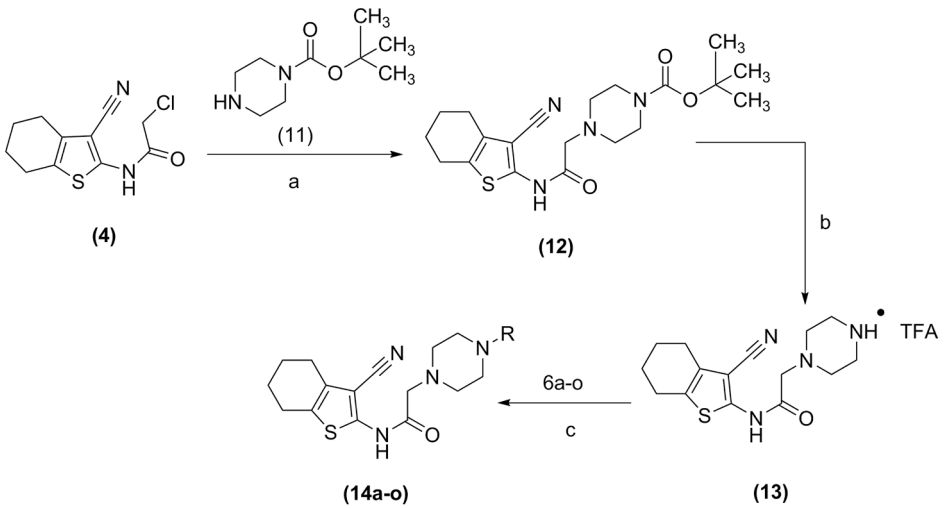

6a = 4-Methylbenzoyl chloride; **6b** = 4-Methoxybenzoyl chloride; **6c** = Benzoyl chloride; **6d** = 4-Chlorobenzoyl chloride; **6e** = 4-Bromobenzoyl chloride; **6f** = Ethyl chlorooxoacetate; **6g** = 4-Nitrobenzoyl chloride; **6h** = Acetyl chloride; **6i** = Benzenesulfonyl chloride; **6j** = 4-Methylbenzylsulfonyl chloride; **6k** = 4-Methoxybenzenesulfonyl chloride; **6l** = 4-Chlorobenzenesulfonyl chloride; **6m** = 2-Thiophenesulfonyl Chloride; **6n** = Methanesulfonyl chloride; **6o** = 4-Fluorobenzenesulfonyl chloride

Scheme 3. Synthetic scheme for the synthesis of *N*-(3-cyano-4,5,6,7-tetrahydrobenzo[*b*]thiophen-2-yl)-2-(piperazin-1-yl)acetamide derivatives (**14a-o**). **Reagents and condition:** (a) K_2CO_3, DMF, 80 °C. 4 h; (b) DCM, TFA, rt, 3 h; (c) TEA, DMF, rt, 30 min.

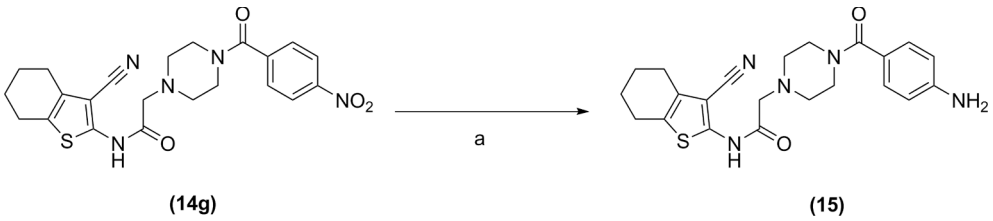

Scheme 4. Synthetic scheme for the synthesis of 2-(4-(4-aminobenzoyl)piperazin-1-yl)-*N*-(3-cyano-4,5,6,7-tetrahydrobenzo[*b*]thiophen-2-yl)acetamide (**15**). **Reagents and condition:** (a) Zn, NH_4Cl, Water, Methanol, 45 °C, 3 h.

Table 1
IC_{50} values describing the effect of representative compounds on HeLa cell nuclear broth.

Compounds	IC_{50} (μM)
9h	1.7 ± 0.12
9o	2.8 ± 0.14
10	2.9 ± 0.13
14i	2.8 ± 0.11
15	3.2 ± 0.09
vorinostat	3.3 ± 0.09

IC_{50} values were determined as the mean ± SD of two independent experiments performed.

enzymes, HDAC4 belongs to class IIa and HDAC6 is a member of class IIb enzymes. Three compounds (**9h**, **9o**, and **14n**) were found active and selective against different HDAC isoforms. These compounds were selected for the determination of IC_{50} values at different concentrations (Table 2) along with three reference standards (vorinostat, trichostatin A, and TMP 269). Compound **9h** was found active against HDAC1 and HDAC6 with an IC_{50} value of 23.2 μM and 33.9 μM, respectively. Compound **9h** displayed 1.46-fold selectivity for HDAC1 over HDAC6 and >4.31-fold selectivity for HDAC1 over HDAC4 (Table 2). Compound **9o** displayed no selectivity and showed week inhibition against HDAC isozymes, however, **14n** displayed selective inhibitory activity against HDAC6 with an IC_{50} value of 13.5 μM against HDAC6 with more than 7.41-fold HDAC6 selectivity over HDAC1 and HDAC4.

2.3.3. *In vitro antiproliferative assay*

Most of the synthesized compounds demonstrated good inhibition against Hela cell nuclear broth. Selected compounds were screened by a more traditional inhibition of cell proliferation (IC_{50}) assay to determine that these compounds can inhibit cancer cell growth. *In vitro* antiproliferative activity of these compounds was assessed against the panel of three different cancer (MDA-MB-231, A549 and HeLa) cell lines. Compounds were screened at several concentrations to obtain a dose-response for calculation of the IC_{50} values. Vorinostat was used as a positive control. Compound **9e** displayed potent activity against breast cancer cell line (MDA-MB- 231) and lung cancer cell line (A549) with an IC_{50} value of 0.31 and 0.02 μM, respectively (Table 3). Other compounds, **15** and **14k** were found active against MDA-MB-231 cell lines, while **9i**, **9o**, **14i,** and **15** were found active against A549 with an IC_{50} value of <0.55 μM (Table 3). In addition, synthesized compounds were also screened against normal human fibroblasts (hTERT RPE-1) to observe the cytotoxicity of these compounds on normal cells. Synthesized compounds were found non-toxic on hTERT RPE-1 cells and did not showed significant inhibition (at least 50%) of the hTERT RPE-1 cells at 50 μM.

Table 2
IC_{50} values describing the effect of representative compounds on HDAC isoform enzymes.

Compound	HDAC1	HDAC4	HDAC6	Selectivity Index			
	IC_{50} (μM)	IC_{50} (μM)	IC_{50} (μM)	1/6	1/4	6/1	6/4
9h	23.2 ± 2.47	>100	33.9 ± 0.80	1.46	>4.31	0.68	>2.95
9o	70.8 ± 1.62	>100	84.7 ± 3.87	1.20	>1.41	0.84	>1.18
14n	45.3 ± 3.43	>100	13.5 ± 0.45	0.30	>2.21	3.36	>7.41
vorinostat	0.065 ± 0.0027	—	0.006 ± 0.00033	0.094	—	10.6	—
trichostatin A	0.003 ± 0.00017	—	0.001 ± 0.00002	0.37	—	2.73	—
TMP 269	—	0.19 ± 0.0015	—	—	—	—	—

IC_{50} values were determined as the mean ± SD of three independent experiments performed.

Table 3
IC_{50} values describing the cytotoxic effects of representative compounds on the panel of three cancer cell lines (MDA- MB-231, A549 and HeLa) and on normal human retina epithelial cell line (hTERT RPE-1).

Compound	MDA- MB-231 IC_{50} (μM)	A549 IC_{50} (μM)	HeLa IC_{50} (μM)	hTERT RPE-1 IC_{50} (μM)
9b	NA	22.79	NA	>50
9e	0.31	0.02	6.65	>50
9h	NA	1.2	4.25	>50
9i	17.28	0.41	9.28	>50
9o	24.25	0.15	23.4	>50
10	NA	7.73	14.4	>50
14e	NA	8.75	13.5	>50
14i	21.29	0.55	16.6	>50
14k	4.84	0.29	12.1	>50
14m	NA	NA	20.3	>50
14n	20.19	0.8	NA	>50
15	2.72	0.15	14.8	>50
vorinostat	7.22	3.26	15.7	>50

IC_{50} values were determined as the mean of three independent experiments performed.
NA = not active at 100 μM.

2.3.4. Analysis of cell death regulation in human cancer cell lines

To investigate the effects of synthesized compounds on cell death induction, we performed fluorescence-activated cell sorting (FACS) analysis, evaluating hypodiploid sub-G1 peak on fixed cells and propidium iodide (PI) incorporation in live cells that reveal DNA fragmentation and dead-cell membrane permeabilization, respectively. The study was performed on two different human cancer cell lines, promonocytic human myeloid leukemia (U937) cells and triple-negative breast cancer (MDA-MB-231) cells. The effect was compared with vorinostat as a reference compound. Compounds **9d**, **9e**, **9o**, and **15** displayed an effect on membrane permeabilization to PI in both the cancer cell lines (Fig. 3). The comparative study revealed that a higher percentage of PI incorporation was observed in U937 cells, which confirmed that this cell line was more sensible for the induction as compared to MDA-MB-231 cells. Compound **9d** showed 25.75% of PI-positive cells in U937; and 10.3% in MDA-MB-231, compound **9e** displayed 11.40% of PI-positive cells in U937 and 9.80% in MDA-MB-231. Similarly, with compound **9o** an effect of 15.1% of PI-positive cells in U937 and 9.7% in MDA-MB-231 was observed; with compound **15**, the percentage of PI-positive cells observed was 8,75% in U937 cells and 11.5% in MDA-MB-231 cells, respectively (Fig. 3A). A different

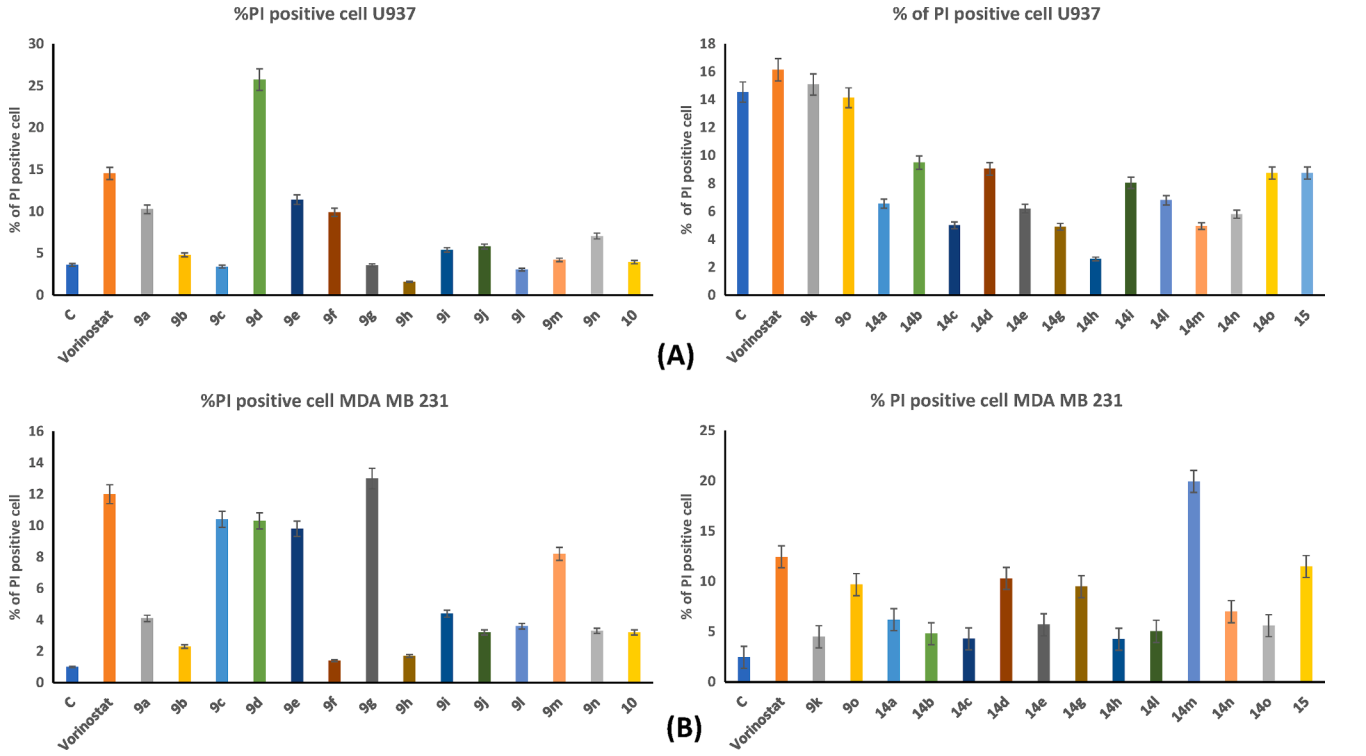

Fig. 3. Evaluation of induction of cell death after treatment with the synthesized compounds using propidium iodide (PI) incorporation in two different cell lines U937 (A) and MDA-MB-231 (B). In brief, cells were harvested with PBS, centrifuged at 1200 rpm for 5 min, and resuspended in 500 μL 1X PBS and 0.2 mg/mL PI. Vorinostat was used as a positive control. Data were acquired using BD Accuri TM C6 flow cytometer system (BD Biosciences). Each experiment was performed in biological triplicates and values expressed as mean ± SD.

response, in terms of "death induction" was observed in both the cancer cell lines used, after the treatment with other compounds. Treatment with compounds **9a**, **9k**, and **14a** in U937 cells, determined a percentage of PI incorporation of 10.25%, 16.15%, and 14.15%, respectively; this effect was comparable to that of vorinostat (14.55%) (Fig. 3A). In MDA-MB-231 breast cancer cells, treatment with **14m,** determined an effect higher compared to that vorinostat; (19.95% *vs* 12.45%, respectively). A lower percentage of cell death was revealed after the induction with compound **9g** (13%) (Fig. 3B).

Concerning the evaluation of DNA fragmentation in U937 cells, compounds **9k** and **14a** led to a strong increase of sub-G1 peak 29.8% and 28.3%, respectively, showing a higher effect than vorinostat (17.6%). (Fig. 4A). With a lower effect, the other compounds **9n** (12.3%), **14c** (12.5%), and **14e** (14.1%) were also found to induce DNA fragmentation (Fig. 4A). A lower DNA fragmentation was observed in MDA-MB-231 cells, confirming that this cell line was more resistant. Only after treatment with compound **14o** a weak increment of the sub-G1 population was observed (8.6%) (Fig. 4B).

2.3.5. *Regulation of cancer cell cycle progression*

The biological effects of newly synthesized compounds were also studied by their capability to regulate cell cycle progression. To discriminate these effects, FACS analysis was performed in the U937 (Fig. 5A) and MDA-MB-231 cell lines (Fig. 5B). In U937 cells, compare to untreated cells (G1, 57.7%; G2/M, 23.9%), a strong reduction of G1 and G2/M phases was observed after induction with compounds **9k** (G1, 42.2%; G2/M, 15.5%), **14a**, (G1, 36.3%; G2/M, 16.8%), and **14g**, (G1, 49.8%; G2/M, 19.9%) (Fig. 5A). A slight reduction of G1 phase was also observed with compounds **9o** (49.6%), **14c** (48.1%), **14d** (51.2%), **14e** (51%), **14h** (51.5%), **14i** (51.2%) and **14m** (51%) (Fig. 5A). A higher percentage of cells in the G1 phase, with respect to control cells (39.2%), was observed with compounds **9g** (46.1%), **9i** (45.8%), and **10** (46%). Treatment with compounds **9b** (23.4%), **9c** (24.7%), **9d** (24%), **9f** (24.5%) and **9g** (23.9%), caused a reduction of cells in G2/M phase. Concerning the S phase, its increments were observed after the treatment with compounds **9b**, **9c**, and **9d** (31.9%, 33.3% and 30.8%, respectively, *vs* 23.7% in control cells) (Fig. 5A) and with compounds **14g**, **14h**, **14i** and **14o** (26.5%, 22.2%, 21.3% and 19.5% respectively, *vs* 12.75% in control cells) (Fig. 5A). In contrast, a strong reduction of the percentage of cells in the S phase was observed with compounds **15** (7.8% *vs* 12.75%), and with compounds **10** and **9n** (18.9% and 14.7% *vs* 23.7% in control cells) (Fig. 5A). Concerning the effects in MDA-MB-231 cells, the strongest variations in the percentage of cells in G1 and S phases were observed after treatment with compounds **9n** (G1, 67.4%; S, 2.3% *vs* G1, 59.8% and S 7.6% in control cells) and **14c** (G1, 59.7%; S, 10.2% *vs* G1, 50.3% and S 17% in control cells). Specifically, these compounds determined an increment of the G1 phase and a reduction of the S phase, compared to control cells (Fig. 5B). A variation in the G1 phase was observed after treatment with other compounds. Particularly, an increment of this phase was observed after treatment with compounds **9k**, **14a**, **14b**, **14e**, and **14h** (59%, 62.4%, 56.5%, 56%, and 56.1%, respectively, *vs* 50.3% in control cells), and with compounds **9h** and **10** (both 64.9% *vs* 59.8% in control cells) (Fig. 5B). A reduction of the percentage of cells in the S phase was observed after treatment with compounds **14d** and **14o** (11.2% and 10%, respectively *vs* 17% in control cells). Moreover, a slight increment in the S phase was revealed after the induction with compounds **9c** (10.8% *vs* 7.6% in control cells) and **9g** (11.7% *vs* 7.6% in control cells) (Fig. 5B). Concerning the G2/M progression, different effects were observed. Specifically, an increment was obtained after treatment with compounds **14l** and **14o** (35.6% and 35%, respectively, *vs* 27.6% in control cells) and a reduction of this cellular phase after stimulation with compounds **9c**, **9d**, **9f**, **9h**, **9j**, **9m** and **10** (24.5%, 24.1%, 25.7%, 25.7%, 20.2%, 21.9%, and 23.6%, respectively, *vs* 30.4% in control cells).

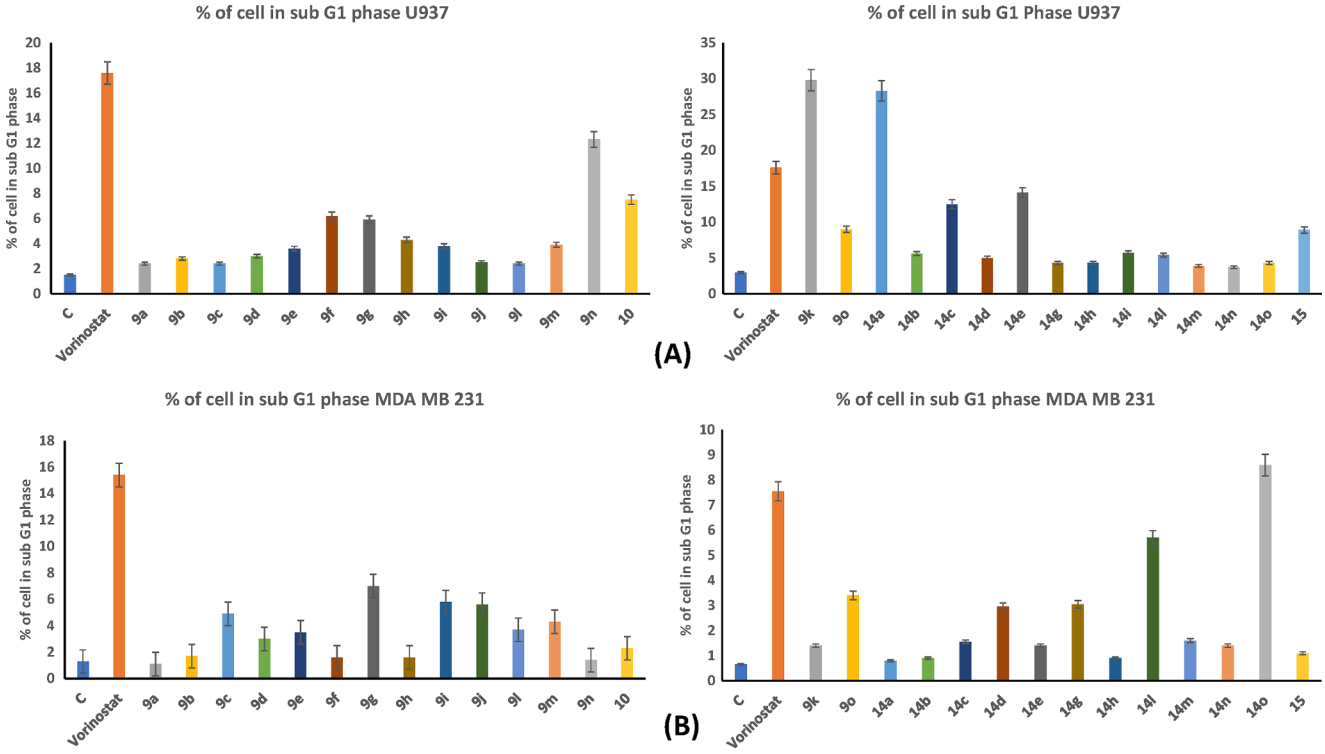

Fig. 4. Evaluation of percentage of cell in sub-G1 phase of cell cycle after treatment with synthesized compounds by FACS analysis in U937 (A) and MDA-MB-231 (B) cell lines. In brief, after stimulation, cell lines were harvested with PBS, centrifuged and resuspended in 500 μL of a hypotonic solution (1X PBS, 0.1% sodium citrate, 0.1% NP-40, freshly added RNAase A, and 50 mg/mL PI). Vorinostat was used as a positive control. Data were acquired using BD Accuri TM C6 flow cytometer system (BD Biosciences). Each experiment was performed in biological triplicates and values expressed as mean ± SD.

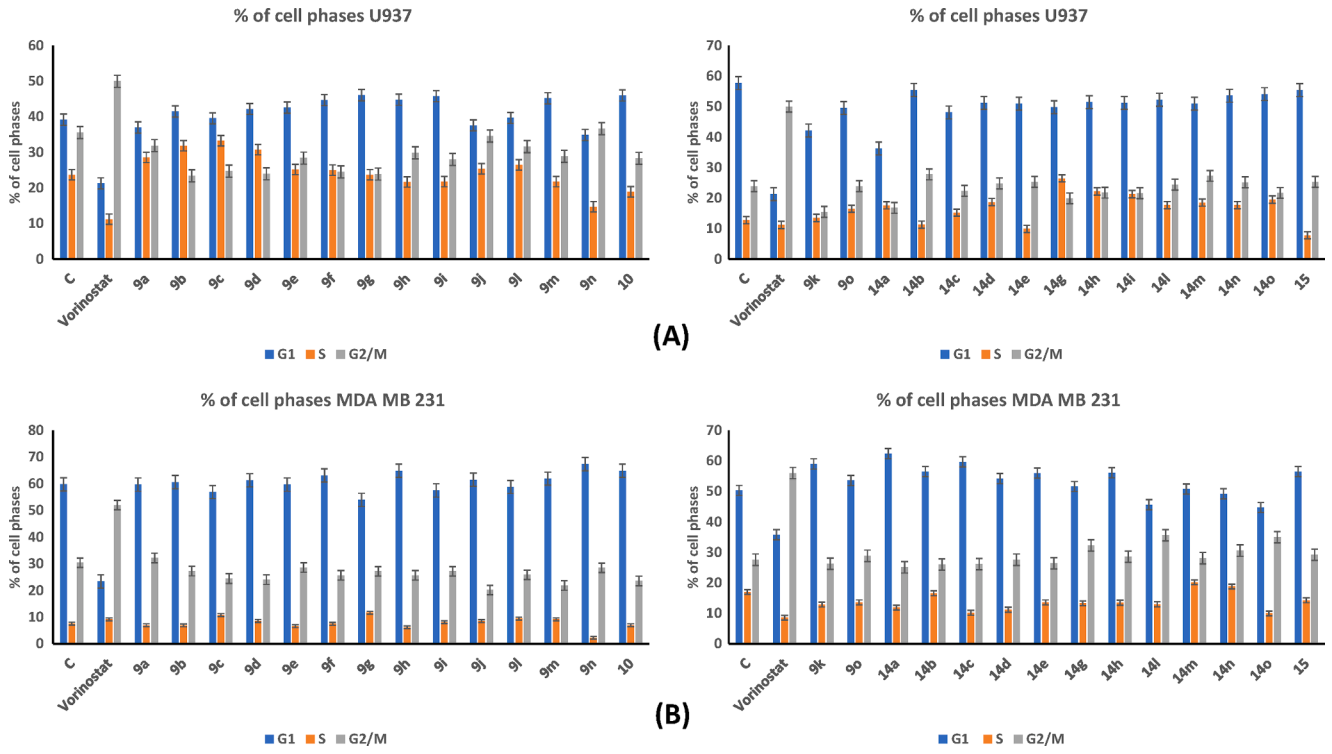

Fig. 5. Evaluation of percentage of cells in G1, S and G2/M phases of cell cycle, after treatment with synthesized compounds by FACS analysis in U937 (A) and MDA-MB-231 (B) cell lines. In brief, after stimulation, cell lines were harvested with PBS, centrifuged and resuspended in 500 µL of a hypotonic solution (1X PBS, 0.1% sodium citrate, 0.1% NP-40, freshly added RNAase A, and 50 mg/mL PI). Vorinostat were used as a positive control. Data were acquired using BD Accuri TM C6 flow cytometer system (BD Biosciences). Each experiment was performed in biological triplicates and values expressed as mean ± SD.

2.3.6. Study of biological function at a molecular level

To extend the study at a molecular level, Western blot analysis was performed. U937 and MDA-MB-231 cells were treated with representative compounds chosen among those that induced cell death or cell cycle alteration, in a specific cell line or in both the cell lines. The biological properties of synthesized compounds were tested for the acetylation levels of histone H3 (lysine K9-14ac) and α-tubulin. H3 and α-tubulin are recognised as molecular targets of class I HDACs and HDAC6 inhibition, respectively. Slow effects in terms of the acetylation status of both the molecular targets were observed after Western blot analysis (Fig. 6A, B). To corroborate the effect on cell cycle progression observed after treatment with selected compounds, a panel of cell cycle-regulating elements were examined. To this aim, a comparative study of cyclin A, D1, and E was performed in U937 (Fig. 6C) and MDA-MB-231cells (Fig. 6D).

A different effect was found between the two cell lines used. In U937, compounds **9k** and **9o** led to a decrease of cyclin A expression; compounds **9d**, **9n**, **9o,** and **14a** caused a significant reduction of cyclin D1 expression, and compounds **9o** and **14a** caused a significant reduction of cyclin E (Fig. 6C). Treatment with compounds **14e** and **15** determined a strong decrease of cyclin A and D1 protein expression, but no variation was observed for cyclin E (Fig. 6C). A different regulation was observed in MDA-MB-231. Particularly, compounds **9k**, **9o**, **14a**, **14e**, and **15** led to an increment of cyclin A, and treatment with compounds **9o** and **14a** caused a decrease of cyclin E protein expression (Fig. 6D). All tested compounds were able to induce a hyperexpression cyclin D1 protein (Fig. 6D).

*2.3.7. In vitro microsomal stability of **9h** and **14n***

For the estimation and prediction of *in vivo* metabolism of these newly synthesized compounds, *in vitro* microsomal stability was performed using LC-MS/MS [21,22]. Metabolic stability was expressed as the percentage (%) of the remaining parent-compound concentration over time with kinetic monitoring. Compounds **9h**, **14n**, and verapamil (standard) were incubated with human (HLM) and rat liver microsomes (RLM) containing cytochrome P450 in the presence of an NADPH generating system. The concentrations of these compounds in microsomal incubations were calculated from their calibration curves. The remaining concentrations (%) were plotted against incubation times (Fig. 7). *In vitro* half-lives ($t_{1/2}$) were determined using Graphpad prism. The *in vitro* half-lives ($t_{1/2}$) were found with HLM in the following ascending order, verapamil < **14n** < **9h**, which is in agreement with the order obtained with RLM (Table 4). However, for **9h**, the results suggested slower metabolism with HLM than with RLM. Among these compounds, **9h** clearly showed better metabolic stability in comparison with that of the reference verapamil (Table 4).

2.4. In silico ADME prediction

ADME properties play a significant role in the determination of the activity and stability of the compounds. We predicted pharmacokinetic and physicochemical properties such as partition coefficient (log $P_{o/w}$), aqueous solubility (log S), molecular weight (MW), hydrogen bod donor (HBD), hydrogen bond acceptor (HBA), total polar surface area (TPSA), molar refractivity (MR), number of rotatable bonds with passive gastrointestinal absorption (GIA), brain penetration (BBB) and cytochromes P_{450} (CYPs) inhibition and compared with vorinostat (**Table S4** under **Electronic Supplementary Information**). All the physicochemical properties were found comparable with vorinostat and found in the acceptable range as per Lipinski's rule of five. GI absorption is a critical parameter for bioavailability, compound **9h** and **14n** demonstrated high GI absorption same as vorinostat. No compounds were predicted with blood brain barrier (BBB) penetration, and some of the synthesized compounds were predicted with inhibition of isoforms of CYPs.

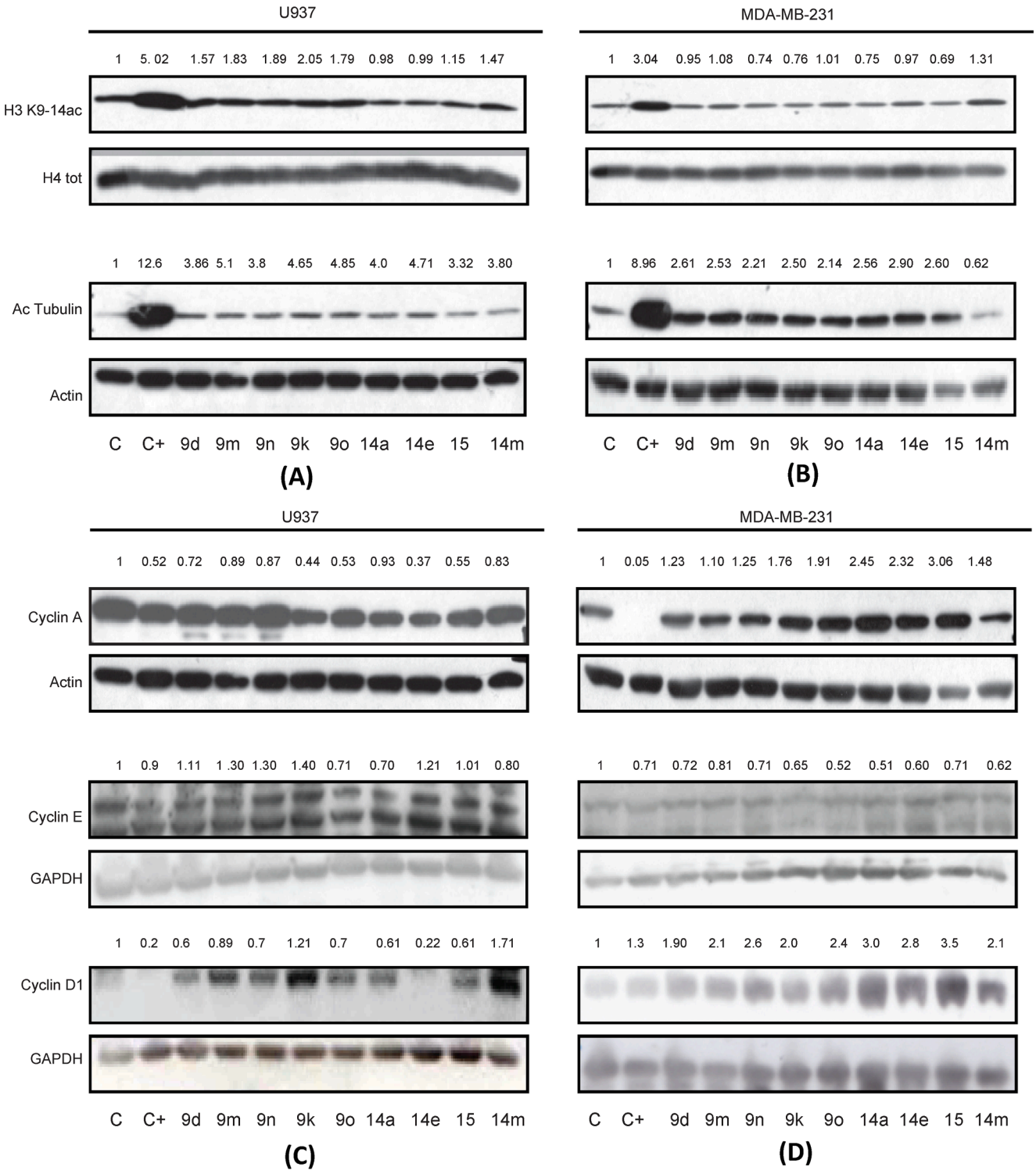

Fig. 6. Effect on synthesized compounds on molecular marker of HDAC (Ac-tubulin and H3 K9-14ac) and cell cycling regulating element (cyclin A, D1 and E) in U937 and MDA-MB-231 cells using western blot analysis. Numbers on western blot indicated the results of the densitometry analysis, performed using the Image J Gel Analysis tool.

2.5. Molecular docking

A molecular docking study was carried out to predict the possible binding orientation of the synthesized compounds with human HDAC6 protein (PDB ID: 5G0G, 1.499 Å). Vorinostat (SAHA®) and trichostatin A were also docked into human HDAC6 to compare the docking results with the synthesized compounds. Hydrogen bond interactions were observed with Gly143, His174, Gly303, and Lys272, while π-π interactions were observed with Phe144 and Trp203 and metal ion interaction with Zn366 in the active site of HDAC6 enzyme (Fig. 8). Docking results were compared with HDAC inhibitory activity of the synthesized compounds and found in agreement with *in vitro* results. Compounds **9h**, **9o**, and **14n** displayed the highest activity among all the synthesized compounds and exhibited the highest docking score of

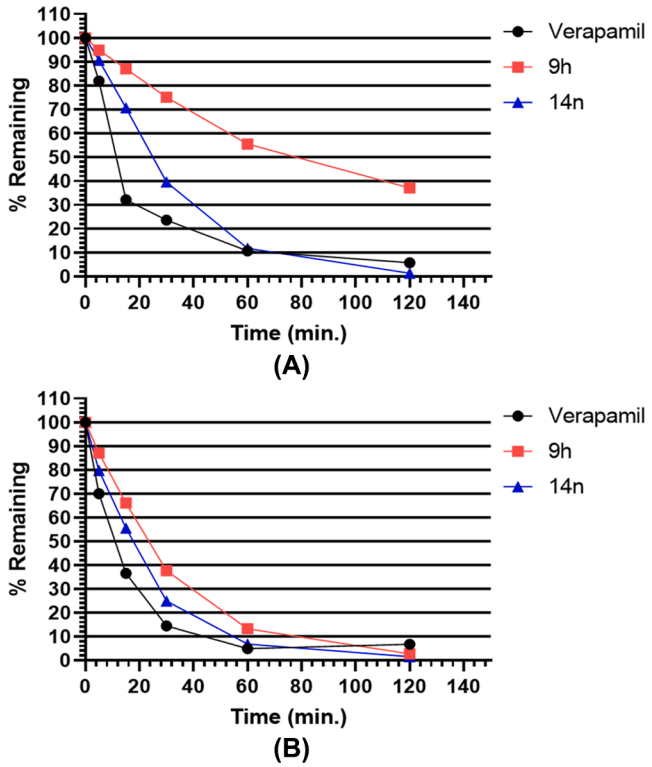

Fig. 7. Metabolic-stability profiles of **9h**, **14n** and verapamil in human liver microsomes (A) and in rat liver microsomes (B).

71.02, 70.40, and 71.97 respectively. Other compounds also showed good docking scores and formed important interactions with the target (**Table S5 Electronic** Supplementary Information). Interactions of these molecules with crucial amino acid residues like Phe144, His174, and Trp203 and metal ion Zinc366 are important and found similar with reference molecules trichostatin A and vorinostat (Fig S2 **Electronic** Supplementary Information).

2.6. Structure-activity relationship (SAR)

To understand SAR, we synthesized two series of tetrahydrobenzo[*b*]thiophene-3-carbonitriles with 16 compounds in each series. Both the series comprised of tetrahydrobenzo[*b*]thiophene-3-carbonitriles as cap group and different substituted amide and sulfonamide as zinc-binding group. Series 1 comprised of piperidin-4-yl-methanamine as linker group and series 2 consisted of piperazine as linker group.

Initially, SAR study was evaluated based on preliminary screening of synthesized compounds at 10 μM on Hela nuclear extract, which is a reach source of HDAC1 and 2. The compounds which showed more than 74% inhibition (**9o**, **9h**, **10**, **14i**, and **15**) were selected for further determination of IC_{50} values and tested at a deferent concentration of (2, 4, 6, 8, and 10 μM). Compound **9h** (IC_{50} = 1.7 ± 0.12 μM), **9o** (IC_{50} = 2.8 ± 0.14 μM), **14i** (IC_{50} = 2.8 ± 0.11 μM) and **15** (IC_{50} = 3.2 ± 0.09 μM) displayed good activity against Hela cell nuclear broth. Next, isoform selectivity assay was performed against HDAC1, HDAC2, HDAC4 and HDAC6 using selected compounds that demonstrated more than 74% inhibition in preliminary screening against Hela nuclear extract. First of all, a preliminary assay was performed at 10 μM concentration with these selected synthesized compounds against HDAC isoforms. Compounds which showed better inhibition against HDAC isoforms were further selected for the determination of IC_{50} values. Compound **9h** with 4-acetyl group at 4th position of linker (piperidin-4-ylmethanamine) was found active against HDAC1 (IC_{50} = 23.2 ± 2.47 μM) and HDAC6 (IC_{50} = 33.9 ± 0.80 μM) amongst the selected compounds. Compound **9o** with 4-fluro-phenyl sulfonamide group at 4th position of linker was found moderately active against HDAC1 (IC_{50} = 70.8 ± 1.62 μM) and HDAC6 (IC_{50} = 84.7 ± 3.87 μM). Compound **14n** with methyl sulfonamide group at 4th position of the linker (piperazine) was found highest active against HDAC1 (IC_{50} = 45.3 ± 3.43 μM) and HDAC6 (IC_{50} = 13.5 ± 0.45 μM) among all the selected compounds. Furthermore, based on these results, it was found that increase in electron-withdrawing characteristics at 4th position of linker leads to decrease in activity *viz.* **9b** with 4-methoxy-benzamide, **14e** with 4-bromo benzamide at 4th position of the linker were found less active against HDAC1 (10.9%), HDAC6 (3.08%) and HDAC1 (4.0%), HDAC6 (4.5%) respectively. Anti-proliferative activity was performed using MTT assay against three different cancer cell lines (MDA-MB-231, A549, and Hela) for selected synthesized compounds (active against Hela nuclear broth). Compound **9e** consisted of 4-bromo-benzamide and compound **14k** with 4-methoxy benzenesulfonamide were found active against all the three cell lines, they demonstrated IC_{50} values of 0.31 μM and 4.84 μM against MDA-MB-231, IC_{50} values of 0.02 μM and 0.29 μM against A549 and IC_{50} values of 6.65 μM and 12.1 μM against Hela cancer cell line, respectively. Compound **9h** was found active against A549 (IC_{50} = 1.2 μM) and Hela (IC_{50} = 4.25 μM) and **9o** was found active against A549 (IC_{50} = 0.15 μM) and moderately active against the rest of the cell lines. Compound **14n** was found highly active against A549 cells (IC_{50} = 0.8 μM).

Based on the above results, it is evident that for isoform selectivity, length of the linker group and bridging moiety play a major role. Finally, it is concluded that the compounds consisted of piperazine linker with aliphatic substitution bridged by sulfonamide moiety displayed better activity against HDAC1 and HDAC6 *viz.* compound **14n**. This suggested that the linker group cannot tolerate the bulky substitution at the 4th position as it may interfere with the entry of molecules in the enzyme pocket, which is evident from the docking study.

3. Conclusion

To summarize, we discovered novel tetrahydrobenzo[*b*]thiophene-3-carbonitrile as histone deacetylase inhibitors. These HDAC inhibitors are consisted of tetrahydrobenzo[*b*]thiophene-3-carbonitrile pharmacophore as cap group, various amide and sulfonamides as ZBG. To understand the SAR, we introduced 4-(aminomethyl) piperidine and piperazine as linker groups. SAR study revealed that less bulky group preferred for substitution at 4th position of linker compared to a bulkier hydrophobic moiety. Variation in the linker group is essential for achieving the desire HDAC selectivity and potency. Compounds **9h** and **14n** with 4-(aminomethyl) piperidine and piperazine groups,

Table 4
Microsomal stabilities of compounds **9h**, **14n** and verapamil.

Compound	Human liver microsomes (HLM)			Rat liver microsomes (RLM)		
	Half Life $t_{1/2}$ (min.)	Intrinsic clearance, Clint (μl/min/mg protein)	Clearance category	Half life $t_{1/2}$ (min.)	Intrinsic clearance, Clint (μl/min/mg protein)	Clearance category
9h	78.50	17.66	medium	21.89	63.32	medium
14n	22.34	62.04	high	15.95	86.90	high
verapamil	9.74	142.36	high	9.18	150.98	high

Metabolic stability is expressed as the *in vitro* half-life time.

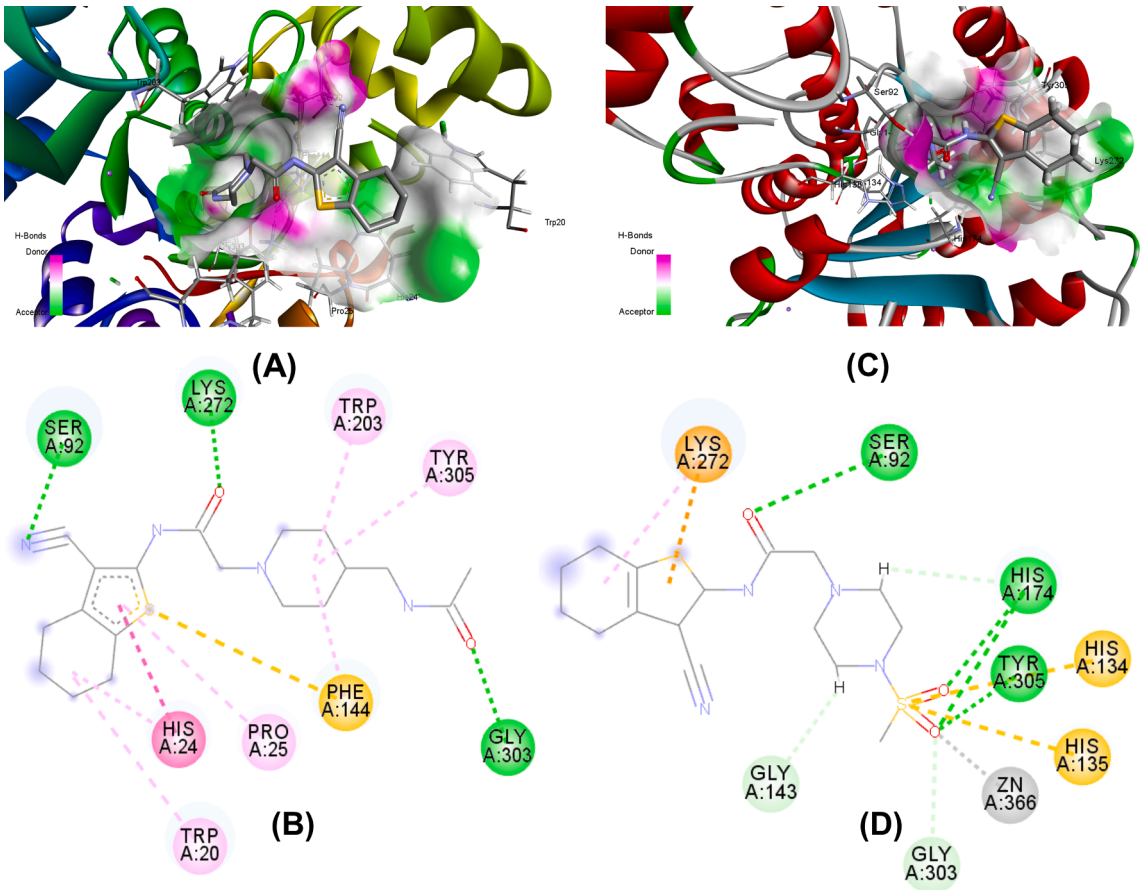

Fig. 8. Binding modes of **9h** and **14n** in the catalytic binding domain of HDAC6 (PDB ID: 5G0G, 1.499 Å). (A) 3D view of **9h** in HDAC6. HDAC6 is rendered in shaded ribbon and **9h** is in stick model with colour by atoms. (B) 2D view of **9h** in HDAC6. Coloured dotted lines represent different binding interactions of **9h** with amino acid residue of HDAC6. **9h** is in wire frame with colour by atoms. (C) 3D view of **14n** in HDAC6. HDAC6 is rendered in shaded ribbon and **14n** is in stick model with colour by atoms. (B) 2D view of **14n** in HDAC6. Coloured dotted lines represent different binding interactions of **14n** with amino acid residue of HDAC6. **14n** is in wire frame with colour by atoms.

respectively, selected for various *in vitro* assays. Both, the compounds displayed micromolar enzymatic potency against HDACs. Compound **9h** and **14n** also exhibited favorable antiproliferative activity in different cancer cell lines and compared with vorinostat. Compound **9o** also showed an effect on target modulation in cancer cells by Western blot analysis. Compounds **9h**, **9o,** and **14n** demonstrated their roles in cell cycle arrest, sub-G1 phase, and also found to induce apoptosis in cancer cell lines. Overall, these analogs exhibited promising activity against isoform-selective HDAC with good potency. This study discovered new molecules as HDAC inhibitors for targeting different cancer *via* the HDAC pathway.

4. Experimental

4.1. Pharmacophore modeling

Eleven molecules (A to K) (Fig. S1 **under Electronic** Supplementary Information) were selected from the literature [23–29] to generate eight pharmacophore models using the DISCOtech module of Sybyl × 1.2 software. The genetic algorithm similarity program (GASP) was used to refine the generated models, which resulted in four refined pharmacophore models (1–4 models). All the parameters were kept as default, except population size (125), mutation weight (96), fitness increment (0.02), and a number of alignment (04). Receiver operating characteristic (ROC) and Günere-Henry (GH) scoring methods were used to validate GSAP generated (refined) pharmacophore models 1–4.

4.2. Chemistry

All the chemicals and solvents were purchased from Avra synthesis, Combi Blocks, Sigma Aldrich, Merck, and Spectrochem and used as purchased. The progress of reaction were monitored on pre-coated TLC plate (Merck TLC Silica gel 60 F_{254}) using *n*-hexane/ethyl acetate and chloroform/methanol as mobile phase. Spots of the reaction mixture on TLC were visualized under ultraviolet radiation (254 nm) chambers. The purification of various intermediates and final compounds was carried out using column chromatography with Merck silica gel 60 M (0.015–0.040 mm) as a stationary phase and the mobile phase mentioned in the specified corresponding experiment. The melting points (mp) of intermediates and final compounds were determined in open capillaries on a digital melting-point apparatus and found uncorrected. ^{1}H and ^{13}C NMR spectra were recorded on a Bruker biospin (Switzerland) Avance III 400 (400.13 MHz for ^{1}H, 100.61 MHz for ^{13}C) using DMSO-d_6 and $CDCl_3$ as solvents. Chemical shifts are given in parts per million (ppm), (relative to tetramethylsilane). HPLC purity was determined on JASCO 4000 system (column isocratic eluent: H_2O/CH_3CN 20:80 (v/v) and H_2O/CH_3CN 30:70 (v/v) flow rate, 1.0 mL/min; UV wavelength, 254–400 nM; temperature, 25 °C; injection volume, 10 μL) over 20 min. The purity of the final compounds of both the series was assessed by HPLC and the purity of all final compounds was found >95% or higher. Mass analysis was performed on EI-MS (20 eV): Agilent Technologies (HP) 5973 mass spectrometer.

*4.2.1. General procedure for synthesis of 2-amino-4,5,6,7-tetrahydrobenzo [b]thiophene-3-carbonitrile **(3)** [30–37]*

A clear two-neck round bottom flask (RBF) was charged with cyclohexanone (**1**) (10.4 mmol) and ethanol (10.0 mL). The resulting solution was cooled at 5 °C. To this reaction mixture (RM), malononitrile (**2**) (10.4 mmol) was added dropwise using a dropping funnel over a period of 5 min, and the resulting solution was stirred at 5 °C for 15 min followed by the addition of elemental sulfur (10.4 mmol) and morpholine (10.4 mmol). The resulting reaction mixture was moved to room temperature. Reaction progress was monitored using TLC. After completion of the reaction, the reaction mixture was poured in cold water, which afforded brownish solid crude product. The isolated solid material was purified by recrystallization using absolute ethanol to give the title compound (**3**) as off-white coloured needle shaped crystal.

*4.2.2. General procedure for synthesis of 2-chloro-N-(3-cyano-4,5,6,7-tetrahydrobenzo[b]thiophen-2-yl) acetamide [38] **(4)***

The solution of 2-amino-4,5,6,7-tetrahydrobenzo[*b*]thiophene-3-carbonitrile) (**3**) (8.4 mmol) in dioxane (15.0 mL) was added to clean three-neck RBF and cooled at 5–10 °C. While maintaining the temperature chloroacetyl chloride (12.6 mmol) was added drop-wise over the period of 10 min by dropping funnel and stirred at 5–10 °C. After complete addition of chloroacetyl chloride, the reaction mixture was moved to room temperature and further stirred for 20 min. Reaction progress was monitored using TLC. After completion of the reaction, the reaction mixture was poured in ice-cold water to afford intermediate **4** as an off-white coloured solid product. Solid intermediate **4** was filtered using Büchner funnel by vacuum filtration, dried under IR lamp, and further purified by trituration using a mixture of diethyl ether: hexane (80:20) as a white powder.

*4.2.3. General procedure for the synthesis of substituted tert-butyl 4-(methylamino) piperidine-1-carboxylate **(7a-o)** [39–41]*

In a dry two necked RBF, equipped with nitrogen source, was charged with solution of commercially available 1-*N*-BOC-4-(aminomethyl)piperidine (**5**) (1.39 mmol) in dichloromethane (DCM) (2.0 mL) and triethylamine (TEA) (2.09 mmol). The resulting reaction mixture was cooled at 10 °C. Commercially available different substituted aromatic and aliphatic acid chlorides and sulphonyl chlorides (**6a-o**) (1.39 mmol) were dissolved in DCM (1.0 mL) and added dropwise to the above solution over the period of 5 min using a glass syringe while maintaining temperature 5–10 °C. Then, the reaction was moved to room temperature after the complete addition of **6a-o** and monitored on TLC. After completion of the reaction, the reaction mixture was concentrated under vacuum to yield semi-solid crude products. Crude products were suspended in a mixture of diethyl ether: hexane (70:30) and cooled at 10 °C. After cooling, products were fall out as white to off-white precipitates and filtered using vacuum filtration. This treatment yields high purity of **7a-o**, used in the next step as obtained.

*4.2.4. General procedure for the synthesis of substituted methenamine N-methyl-1-(piperidin-4-yl) **(8a–o)** [42]*

Different substitute aliphatic and aromatic amides and sulphonamides (**7a-o)** were added to clean RBF and dissolved in DCM (5.0 mL), which was followed by the addition of trifluoroacetic acid (TFA) (3.0 eq). The resulting reaction was stirred at room temperature until completion of reaction and progress was monitored on TLC. After completion of the reaction, the mixture was concentrated under a vacuum to yield crude products in gummy form. The crude products were purified by washing with diethyl ether (5 mL × 82). After washing, products (**8a-o**) were obtained as white to off-white free-flowing powder and used in the next step as obtained.

*4.2.5. General procedure for synthesis of substituted 2-(4-(aminomethyl) piperidin-1-yl)-N-(3-cyano-4,5,6,7-tetrahydrobenzo[b]thiophen-2-yl) acetamide **(9a-o)** [43]*

A two-neck RBF was charged with a solution of intermediate **4** (0.78 mmol) in dioxane (3 mL) and triethylamine (TEA) (2.35 mmol). The reaction mixture was stirred at room temperature for 10 min, followed by the addition of respective **8a-o** (0.78 mmol). Then the reaction was move to 70 °C and stirred until the completion of the reaction. The progress of the reaction was monitored on TLC, after completion of the reaction, the temperature was brought to the normal temperature, and the reaction mixture was poured into ice-cold water. Precipitates were obtained and collected using vacuum filtration and dried. The crude products were purified by column chromatography and/or trituration using diethyl ether.

*4.2.5.1. N-((1-(2-((3-cyano-4,5,6,7-tetrahydrobenzo[b]thiophen-2-yl) amino)-2-oxoethyl)piperidin-4-yl)methyl)-4-methylbenzamide **(9a)**.* Compound **9a** was synthesized as per general procedure described above as off-white solid in the yield of 75%, mp 235–237 °C. ^{1}H NMR (400 MHz, DMSO-d_6) : δ 10.91–10.88 (t, J = 11.6, 1H), 8.43 (s, 1H), 7.76–7.74 (d, J = 8, 2H), 7.26–7.24 (d, J = 7.6, 2H), 3.28 (s, 2H), 3.16–3.13 (t, J = 12, 2H), 2.91–2.88 (d. J = 10.4, 2H), 2.58 (s, 3H), 2.34 (s, 3H), 2.23–2.18 (t, J = 22, 2H), 1.74–1.68 (m, 7H), 1.58 (s, 1H), 1.30–1.17 (m, 2H); ^{13}C NMR (100 MHz, DMSO-d_6): δ 167.9, 166.0, 140.7, 131.7, 130.3, 128.7, 127.1, 114.2, 60.1, 54.9, 52.8, 44.5, 40.0, 35.0, 29.7, 23.4, 23.3, 22.5, 21.6, 20.9. MS (ESI) calcd for $C_{25}H_{30}N_4O_2S$ [M^+] 450.21; found: 451.21 [M+H]. HPLC analysis: retention time = 6.360 min; peak area = 97.63%; eluent A, ACN; eluent B, H_2O; isocratic (80:20) over 20 min with a flow rate of 1 mL min^{-1}.

*4.2.5.2. N-((1-(2-((3-cyano-4,5,6,7-tetrahydrobenzo[b]thiophen-2-yl) amino)-2-oxoethyl)piperidin-4-yl)methyl)-4-methoxybenzamide **(9b)**.* Compound **9b** was synthesized as per general procedure described above as dull white solid in the yield of 70%, mp 190–193 °C. ^{1}H NMR (400 MHz, $CDCl_3$): δ 10.48 (bs, 1H), 7.78–7.76(d, J = 8, 2H), 6.93–6.90 (d, J = 12, 2H), 6.47 (s, 1H), 3.84 (s, 3H), 3.37 (s, 2H), 3.19 (s, 2H), 2.92–2.89 (d, J = 12, 2H), 2.63–2.59 (d, J = 16, 3H), 2.43–2.40 (m, 3H),1.80–1.74 (m, 6H), 1.53–1.44 (m, 3H); ^{13}C NMR (100 MHz, $CDCl_3$): δ 167.6, 166.2, 162.1, 146.4, 130.7, 128.7, 128.1, 126.8, 114.2, 113.7, 93.8, 60.7, 55.4, 53.8, 45.1, 35.0, 30.2, 24.07, 24.02, 23.1, 22.1. MS (ESI) calcd for $C_{25}H_{30}N_4O_3S$ [M^+] 466.20; found: 467.30 [M+H]. HPLC analysis: retention time = 5.683 min; peak area = 97.46%; eluent A, ACN; eluent B, H_2O; isocratic (80:20) over 20 min with a flow rate of 1 mL min^{-1}. Crude compound was purified using column chromatography using *n*-Hexane and ethyl acetate as an eluent.

*4.2.5.3. N-((1-(2-((3-cyano-4,5,6,7-tetrahydrobenzo[b]thiophen-2-yl) amino)-2-oxoethyl)piperidin-4-yl)methyl)benzamide **(9c)**.* Compound **9c** was synthesized as per general procedure described above as white solid in the yield of 73%, mp 194–196 °C. ^{1}H NMR (400 MHz, $CDCl_3$): δ 10.76 (bs, 1H), 7.81–7.80 (d, J = 4, 2H), 7.51–7.47 (m, 1H), 7.44–7.40 (m, 2H), 6.65–6.61 (t, J = 16, 1H), 3.40–3.37 (t, J = 12, 3H), 3.19 (s, 2H), 2.92–2.89 (d, J = 12, 2H), 2.63–2.59 (d, J = 16, 4H), 2.36–2.30 (t, J = 24, 2H) 1.85–1.72 (m, 6H), 1.50–1.44 (m, 2H); ^{13}C NMR (100 MHz, $CDCl_3$): δ 167.7, 167.6, 146.3, 134.5, 131.4, 130.7, 128.5, 128.1, 127.0, 114.2, 93.8, 60.7, 53.8, 45.2, 35.0, 30.2, 29.8, 24.07, 24.01, 23.1, 22.1. MS (ESI) calcd for $C_{24}H_{28}N_4O_2S$ [M^+] 436.19; found: 437.20 [M+H]. HPLC analysis: retention time = 5.590 min; peak area = 95.07%; eluent A, ACN; eluent B, H_2O; isocratic (80:20) over 20 min with a flow rate of 1 mL min^{-1}.

*4.2.5.4. 4-Chloro-N-((1-(2-((3-cyano-4,5,6,7-tetrahydrobenzo[b]thiophen-2-yl)amino)-2-oxoethyl) piperidin-4-yl)methyl)benzamide **(9d)**.* Compound **9d** was synthesized as per general procedure described above as brownish white solid in the yield of 80%, mp 210–212 °C. ^{1}H

NMR (400 MHz, $CDCl_3$): δ 10.56 (bs, 1H), 7.77–7.74 (d, J = 12, 2H), 7.41–7.39 (d, J = 12, 2H), 6.67 (s, 1H), 3.51–3.47 (m, 1H), 3.41–3.38 (t, J = 12, 2H), 3.20 (s, 2H), 2.93–2.90 (d, J = 12, 2H), 2.64–2.60 (d, J = 16, 3H), 2.38–2.32 (t, J = 24, 2H) 1.80–1.74 (m, 6H), 1.55–1.46 (m, 2H), 1.29–1.19 (m, 1H); ^{13}C NMR (100 MHz, $CDCl_3$): δ 167.5, 166.8, 146.4, 137.6, 132.9, 130.7, 128.7, 128.5, 128.2, 114.3, 93.7, 65.8, 60.7, 53.7, 45.1, 34.9, 30.1, 29.8, 24.0, 23.1, 22.1, 15.2. MS (ESI) calcd for $C_{24}H_{27}ClN_4O_2S$ [M^+] 470.15; found: 471.20 [M+H], 473.30 [M+2]. HPLC analysis: retention time = 6.763 min; peak area = 95.22%; eluent A, ACN; eluent B, H_2O; isocratic (80:20) over 20 min with a flow rate of 1 mL min^{-1}.

*4.2.5.5. 4-Bromo-N-((1-(2-((3-cyano-4,5,6,7-tetrahydrobenzo[b]thiophen-2-yl)amino)-2-oxoethyl) piperidin-4-yl)methyl)benzamide **(9e)**.* Compound **9e** was synthesized as per general procedure described above as off white solid in the yield of 70%, mp 215–217 °C. ^{1}H NMR (400 MHz, $CDCl_3$): δ 10.56 (bs, 1H), 7.77–7.74 (d, J = 12, 2H), 7.41–7.39 (d, J = 12, 2H), 6.67 (s, 1H), 3.51–3.47 (m, 1H), 3.41–3.38 (t, J = 12, 2H), 3.20 (s, 2H), 2.93–2.90 (d, J = 12, 2H), 2.64–2.60 (d, J = 16, 3H), 2.38–2.32 (t, J = 24, 2H) 1.80–1.74 (m, 6H), 1.55–1.46 (m, 2H), 1.29–1.19 (m, 1H); ^{13}C NMR (100 MHz, $CDCl_3$) : δ 167.5, 166.8, 146.4, 137.6, 132.9, 130.7, 128.7, 128.5, 128.2, 114.3, 93.7, 65.8, 60.7, 53.7, 45.1, 34.9, 30.1, 29.8, 24.0, 23.1, 22.1, 15.2. MS (ESI) calcd for $C_{24}H_{27}BrN_4O_2S$ [M^+] 514.10; found: 515.10 [M+H], 517.10 [M+2]. HPLC analysis: retention time = 11.510 min; peak area = 100%; eluent A, ACN; eluent B, H_2O; isocratic (70:30) over 20 min with a flow rate of 1 mL min^{-1}.

*4.2.5.6. Ethyl 2-(((1-(2-((3-cyano-4,5,6,7-tetrahydrobenzo[b]thiophen-2-yl)amino)-2-oxoethyl) piperidin-4-yl)methyl)amino)-2-oxoacetate **(9f)**.* Compound **9f** was synthesized as per general procedure described above as white solid in the yield of 85%, mp 141–143 °C. ^{1}H NMR (400 MHz, $CDCl_3$): δ 10.45 (bs, 1H), 7.37–7.34 (t, J = 12, 1H), 4.38–4.33 (q, J = 12, 8, 2H), 3.31–3.28 (t, J = 12, 2H), 3.21 (s, 2H), 2.94–2.91 (d, J = 12, 2H), 2.65–2.57 (dt, J = 8, 8 4H), 2.37–2.30 (td, J = 4, 12, 2H) 1.88–1.78 (m, 6H), 1.68 (s, 1H), 1.51–1.44 (m, 2H), 1.40–1.36 (t, J = 16, 3H); ^{13}C NMR (100 MHz, $CDCl_3$): δ 167.4, 160.7, 156.8, 146.2, 130.7, 128.1, 114.1, 93.8, 63.2, 60.7, 53.6, 45.0, 34.8, 31.6, 30.0, 29.6, 24.0, 23.9, 23.1, 22.1, 13.9. MS (ESI) calcd for $C_{21}H_{28}N_4O_4S$ [M^+] 432.18; found: 455 [M+Na], 431 [M−H]. HPLC analysis: retention time = 4.917 min; peak area = 96.291%; eluent A, ACN; eluent B, H_2O; isocratic (80:20) over 20 min with a flow rate of 1 mL min^{-1}.

*4.2.5.7. N-((1-(2-((3-cyano-4,5,6,7-tetrahydrobenzo[b]thiophen-2-yl) amino)-2-oxoethyl)piperidin-4-yl)methyl)-4-nitrobenzamide **(9g)**.* Compound **9g** was synthesized as per general procedure described above as yellowish solid in the yield of 75%, mp 158–160 °C. ^{1}H NMR (400 MHz, $CDCl_3$): δ 10.61 (bs, 1H), 8.30–8.28 (d, J = 8, 2H), 8.01–7.99 (d, J = 8, 2H), 6.69–6.66 (t, J = 12, 1H), 3.48–3.46 (t, J = 8, 2H), 3.22 (s, 2H), 2.96–2.93 (d, J = 12, 2H), 2.65–2.58 (m, 4H), 2.42–2.36 (td, J = 4, 12, 2H) 1.87–1.76 (m, 6H), 1.62–1.52 (m, 2H), 1.30–1.26 (m, 1H); ^{13}C NMR (100 MHz, $CDCl_3$): δ 167.4, 165.9, 149.5, 146.5, 140.1, 130.7, 128.3, 128.2, 123.7, 114.4, 93.7, 60.6, 53.7, 45.2, 34.9, 31.5, 30.0, 24.09, 24.04, 23.1, 22.6, 22.0, 14.1. MS (ESI) calcd for $C_{24}H_{27}N_5O_4S$ [M^+] 481.18; found: 482.30 [M+H]. HPLC analysis: retention time = 5.530 min; peak area = 96.812%; eluent A, ACN; eluent B, CH_3OH; isocratic (80:20) over 20 min with a flow rate of 1 mL min^{-1}.

*4.2.5.8. 2-(4-(Acetamidomethyl)piperidin-1-yl)-N-(3-cyano-4,5,6,7-tetrahydrobenzo[b]thiophen-2-yl)acetamide **(9h)**.* Compound **9h** was synthesized as per general procedure described above as white solid in the yield of 90%, mp 190–192 °C. ^{1}H NMR (400 MHz, $CDCl_3$): δ 10.67 (bs, 1H), 5.79–5.76 (t, J = 12, 1H), 3.28–3.20 (m, 4H), 2.92–2.87 (m, 2H), 2.66–2.59 (dt, J = 8, 12, 4H), 2.39–2.33 (td, J = 8, 2H), 2.03–2.01 (s, 3H) 1.87–1.83 (m, 4H), 1.80–1.76 (m, 2H), 1.67–1.61 (m, 1H), 1.60–1.43 (m, 2H); ^{13}C NMR (100 MHz, $CDCl_3$): δ 170.6, 167.6, 146.5, 130.7, 128.1, 114.3, 93.7, 60.5, 53.7, 44.5, 34.7, 30.0, 29.4, 24.07, 24.00, 23.2, 23.0, 22.0. MS (ESI) calcd for $C_{19}H_{26}N_4O_2S$ [M^+] 374.18; found: 375.50 [M+H]. HPLC analysis: retention time = 5.393 min; peak area = 95.23%; eluent A, ACN; eluent B, H_2O; isocratic (80:20) over 20 min with a flow rate of 1 mL min^{-1}.

*4.2.5.9. N-(3-cyano-4,5,6,7-tetrahydrobenzo[b]thiophen-2-yl)-2-(4-(phenylsulfonamidomethyl) piperidin-1-yl)acetamide **(9i)**.* Compound **9i** was synthesized as per general procedure described above as off white solid in the yield of 87%, mp 185–187 °C. ^{1}H NMR (400 MHz, $CDCl_3$): δ 10.41 (bs, 1H), 7.78–7.86 (d, J = 8, 2H), 7.61–7.57 (m, 1H), 7.55–7.51 (m, 2H), 5.01–4.97 (t, J = 12, 1H), 3.25–3.18 (m, 3H), 2.88–2.85 (m, 5H), 2.64–2.57 (dt, J = 4, 8, 4H), 2.30–2.25 (t, J = 8, 2H), 1.83–1.73 (m, 4H), 1.57–1.50 (m, 1H), 1.39–1.29 (m, 2H); ^{13}C NMR (100 MHz, $CDCl_3$): δ 167.5, 146.3, 139.9, 132.6, 130.7, 129.1, 128.2, 126.9, 114.2, 93.8, 60.6, 53.6, 48.3, 35.4, 29.9, 24.07, 24.01, 23.1, 22.1. MS (ESI) calcd for $C_{23}H_{28}N_4O_3S_2$ [M^+] 472.16; found: 473.3 [M+H]. HPLC analysis: retention time = 5.563 min; peak area = 96.14%; eluent A, ACN; eluent B, H_2O; isocratic (80:20) over 20 min with a flow rate of 1 mL min^{-1}.

*4.2.5.10. N-(3-cyano-4,5,6,7-tetrahydrobenzo[b]thiophen-2-yl)-2-(4-((((4-methylphenyl)sulfonamido)methyl)piperidin-1-yl)acetamide **(9j)**.* Compound **9j** was synthesized as per general procedure described above as white solid in the yield of 95%), mp 182–184 °C. ^{1}H NMR (400 MHz, $CDCl_3$): δ 10.25 (bs, 1H), 7.76–7.74 (d, J = 8, 2H), 7.32–7.30 (d, J = 8, 2H), 5.04 (s, 1H), 3.25–3.18 (m, 2H), 2.92–2.82 (m, 4H), 2.64–2.57 (dt, J = 4, 8, 4H), 2.43 (s, 3H), 2.33–2.24 (td, J = 8, 12, 2H), 1.83–1.73 (m, 6H), 1.58–1.59 (m, 1H), 1.41–1.28 (m, 2H); ^{13}C NMR (100 MHz, $CDCl_3$): δ 167.5, 146.3, 143.3, 136.9, 130.7, 129.7, 128.2, 127.0, 114.2, 93.7, 60.6, 53.6, 48.3, 35.4, 29.9, 24.07, 24.01, 23.1, 22.1. MS (ESI) calcd for $C_{24}H_{30}N_4O_3S_2$ [M^+] 486.18; found: 487.3 [M+H]. HPLC analysis: retention time = 6.077 min; peak area = 95.185%; eluent A, ACN; eluent B, H_2O; isocratic (80:20) over 20 min with a flow rate of 1 mL min^{-1}. Crude compound was purified using column chromatography using *n*-Hexane and ethyl acetate as an eluent.

*4.2.5.11. N-(3-cyano-4,5,6,7-tetrahydrobenzo[b]thiophen-2-yl)-2-(4-((((4-methoxyphenyl) sulfonamido)methyl)piperidin-1-yl)acetamide **(9k)**.* Compound **9k** was synthesized as per general procedure described above as off white solid in the yield of 80%, mp 210–212 °C. ^{1}H NMR (400 MHz, $CDCl_3$): δ 10.43 (bs, 1H), 7.81–7.79 (d, J = 8, 2H), 7.00–6.98 (d, J = 8, 2H), 4.71–4.68 (t, J = 4, 12, 1H), 3.88 (s, 3H), 3.19 (s, 2H), 2.88–2.83 (m, 4H), 2.65–2.58 (m, 4H), 2.32–2.26 (td, J = 8, 12, 2H), 1.83–1.72 (m, 5H), 1.77–1.73 (m, 2H), 1.55–1.52 (m, 1H), 1.39–1.33 (m, 2H); ^{13}C NMR (100 MHz, $CDCl_3$) : δ 167.5, 162.8, 146.3, 131.5, 130.7, 129.1, 128.2, 114.2, 93.7, 60.7, 55.6, 53.6, 48.3, 35.4, 29.9, 24.07, 24.01, 23.1, 22.1. MS (ESI) calcd for $C_{24}H_{30}N_4O_4S_2$ [M^+] 502.17; found: 503.3 [M+H]. HPLC analysis: retention time = 5.683 min; peak area = 95.57%; eluent A, ACN; eluent B, H_2O; isocratic (80:20) over 20 min with a flow rate of 1 mL min^{-1}.

*4.2.5.12. 2-(4-(((4-Chlorophenyl)sulfonamido)methyl)piperidin-1-yl)-N-(3-cyano-4,5,6,7-tetrahydrobenzo[b]thiophen-2-yl)acetamide **(9l)**.* Compound **9l** was synthesized as per general procedure described above as yellowish white solid in the yield of 75%, mp 162–164 °C. ^{1}H NMR (400 MHz, $CDCl_3$): δ 10.42 (bs, 1H), 7.82–7.80 (d, J = 8, 2H), 7.50–7.48 (d, J = 8, 2H), 5.23 (s, 1H), 3.19 (s, 2H), 2.88–2.86 (m, 4H), 2.63–2.58 (m, 4H), 2.32–2.26 (m, 2H), 1.76–1.73 (m, 6H), 1.54 (s, 1H), 1.40–1.25 (m, 2H); ^{13}C NMR (100 MHz, $CDCl_3$): δ 167.5, 146.3, 139.0, 138.5, 130.7, 129.4, 128.5, 128.2, 114.2, 93.7, 60.6, 53.5, 48.3, 35.4, 29.9, 24.07, 24.01, 23.1, 22.1. MS (ESI) calcd for $C_{23}H_{27}ClN_4O_3S_2$ [M^+] 506.12; found: 506.67 [M+], 508.67 [M+2]. HPLC analysis: retention time = 6.493 min; peak area = 97.38%; eluent A, ACN; eluent B, H_2O; isocratic (80:20) over 20 min with a flow rate of 1 mL min^{-1}.

4.2.5.13. N-(3-cyano-4,5,6,7-tetrahydrobenzo[b]thiophen-2-yl)-2-(4-((thiophene-2-sulfonamido) methyl)piperidin-1-yl)acetamide ***(9m)***. Compound **9m** was synthesized as per general procedure described above as brown solid in the yield of 65%, mp 120–122 °C. ^{1}H NMR (400 MHz, $CDCl_3$): δ 10.31 (bs, 1H), 7.72–7.54 (m, 2H), 7.11–7.09 (m, 1H), 5.17 (s, 1H), 3.20 (s, 2H), 2.96–2.87 (dd, J = 8, 24, 4H), 2.64–2.57 (dt, J = 4, 8, 4H), 2.33–2.28 (m, 2H), 1.83–1.77 (m, 6H), 1.55 (s, 1H), 1.42–1.29 (m, 2H); ^{13}C NMR (100 MHz, $CDCl_3$): δ 167.5, 146.3, 140.9, 132.0, 131.7, 130.7, 128.2, 127.4, 114.2, 93.8, 60.7, 53.6, 48.6, 35.3, 29.9, 24.07, 24.01, 23.1, 22.1. MS (ESI) calcd for $C_{21}H_{26}N_4O_3S_3$ [M^+] 478.12; found: 479.3 [M+H]. HPLC analysis: retention time = 5.377 min; peak area = 97.89%; eluent A, ACN; eluent B, H_2O; isocratic (80:20) over 20 min with a flow rate of 1 mL min^{-1}.

4.2.5.14. N-(3-cyano-4,5,6,7-tetrahydrobenzo[b]thiophen-2-yl)-2-(4-(methylsulfonamidomethyl) piperidin-1-yl)acetamide ***(9n)***. Compound **9n** was synthesized as per general procedure described above as white solid in the yield of 95%, mp 181–183 °C. ^{1}H NMR (400 MHz, $CDCl_3$): δ 10.48 (bs, 1H), 4.62–4.59 (t, J = 12, 1H), 3.22 (s, 2H), 3.10–3.07 (t, J = 12, 2H), 2.98 (s, 3H), 2.94–2.91(m, 2H), 2.65–2.58 (dt, J = 4, 8, 4H), 2.39–2.33 (m, 2H), 1.85–1.81 (m, 6H), 1.64–1.59 (m, 1H), 1.51–1.43 (m, 2H); ^{13}C NMR (100 MHz, $CDCl_3$): δ 167.5, 146.4, 130.7, 128.2, 114.3, 93.7, 60.6, 53.6, 48.3, 40.2, 35.7, 29.9, 24.08, 24.01, 23.1, 22.1. MS (ESI) calcd for $C_{18}H_{26}N_4O_3S_2$ [M^+] 410.14; found: 411.3 [M+H]. HPLC analysis: retention time = 4.350 min; peak area = 95.20%; eluent A, ACN; eluent B, H_2O; isocratic (80:20) over 20 min with a flow rate of 1 mL min^{-1}.

4.2.5.15. N-(3-cyano-4,5,6,7-tetrahydrobenzo[b]thiophen-2-yl)-2-(4-(((4-fluorophenyl)sulfonamido) methyl)piperidin-1-yl)acetamide ***(9o)***. Compound **9o** was synthesized as per general procedure described above as off white solid in the yield of 87%, mp 174–176 °C. ^{1}H NMR (400 MHz, $CDCl_3$): δ 10.19 (bs, 1H), 7.91–7.87 (m, 2H), 7.22–7.18 (m, 2H), 5.05 (s, 1H), 3.19 (s, 2H), 2.9–2.87 (m, 4H), 2.64–2.59 (m, 4H), 2.32–2.27 (m, 2H), 1.83–1.82(m, 4H), 1.76–1.72 (m, 2H),1.54 (s, 1H), 1.38–1.35 (m, 2H); ^{13}C NMR (100 MHz, $CDCl_3$): δ 167.5, 166.2, 163.7, 146.4, 136.1, 130.7, 129.79, 129.7, 128.2, 116.4, 116.2, 114.2, 93.7, 60.6, 53.8, 53.6, 48.3, 35.4, 29.9, 24.07, 24.00, 23.0, 22.0. MS (ESI) calcd for $C_{23}H_{27}FN_4O_3S_2$ [M^+] 490.15; found: 491.3 [M+H]. HPLC analysis: retention time = 5.623 min; peak area = 96.52%; eluent A, ACN; eluent B, H_2O; isocratic (80:20) over 20 min with a flow rate of 1 mL min^{-1}.

4.2.6. General procedure for the synthesis of 4-amino-N-((1-(2-((3-cyano-4,5,6,7-tetrahydrobenzo[b]thiophen-2-yl)amino)-2-oxoethyl)piperidin-4-yl)methyl)benzamide ***(10)*** *[44,45]*

In a clean RBF, **9g** was added (0.47 mmol), in a mixture of methanol (4.0 mL) and water (2.0 mL). To the resulting reaction mixture, dry activated zinc (2.35 mmol) was added, which was followed by the addition of NH_4Cl (2.35 mmol). The resulting reaction mixture was stirred at 45 °C until the completion of the reaction. Progress of the reaction was monitored using TLC. After completion of the reaction, the reaction mixture was poured into ice-cold water and extracted with ethyl acetate (10 mL × 3). The combined organic layer was dried over anhydrous Na_2SO_4 and concentrated in vacuo. Crude **10** was purified by column chromatography using hexane: ethyl acetate (70:30) as a mobile phase.

4.2.6.1. 4-Amino-N-((1-(2-((3-cyano-4,5,6,7-tetrahydrobenzo[b]thiophen-2-yl)amino)-2-oxoethyl) piperidin-4-yl)methyl)benzamide ***(10)***. Compound **10** was synthesized as per general procedure described above as off white solid in the yield of 65%, mp 258–260 °C. ^{1}H NMR (400 MHz, DMSO-d_6): δ 10.82 (bs, 1H), 8.04–8.02 (t, J = 8, 1H), 7.57–7.55 (d, J = 8, 2H), 6.53–6.51 (d, J = 8, 2H), 5.59 (s, 2H), 3.11–3.09 (t, J = 8, 2H), 2.91–2.87 (m, 2H), 2.60–2.57 (m, 2H), 2.49 (s, 4H), 2.23–2.17 (td, J = 4, 12, 2H) 1.78–1.73 (m, 4H), 1.70–1.66 (m, 2H), 1.59–1.49 (m, 1H), 1.28–1.18 (m, 2H); ^{13}C NMR (100 MHz, DMSO-d_6): δ 167.9, 166.2, 151.4, 147.0, 130.3, 128.6, 127.1, 121.3, 114.2, 112.4, 92.9, 60.2, 52.9, 44.4, 40.0, 38.8, 35.1, 29.8, 23.46, 23.40, 22.6, 21.6. MS (ESI) calcd for $C_{24}H_{29}N_5O_2S$ [M^+] 451.20; found: 452.30 [M+H]. HPLC analysis: retention time = 6.077 min; peak area = 96.13%; eluent A, ACN; eluent B, H_2O; isocratic (80:20) over 20 min with a flow rate of 1 mL min^{-1}.

4.2.7. General procedure for the synthesis of tert-butyl 4-(2-((3-cyano-4,5,6,7-tetrahydrobenzo[b]thiophen-2-yl)amino)-2-oxoethyl)piperazine-1-carboxylate ***(12)*** *[43,46]*

In a clean and dry three-necked RBF, a solution of commercially available 1-*N*-BOC-piperidine (**11**) (26.8 mmol) in DMF (60.0 mL) was added and stirred at room temperature. Followed by the addition of intermediate **4** (26.8 mmol) and K_2CO_3 (80 mmol). The reaction was moved to 80 °C and stirred until the completion. The progress of the reaction was monitored on TLC. After completion of the reaction, the temperature was brought to room temperature and the reaction mixture was poured into ice-cold water. The precipitates were collected using vacuum filtration and dried using IR lamp. The crude product was washed with a mixture of diethyl ether: hexane (70:30) (10 mL × 3). This treatment resulted in off-white powdered **12** and collected using a vacuum filter. This yields high purity of **12,** which was used in the next step.

4.2.8. General procedure for the synthesis of N-(3-cyano-4,5,6,7-tetrahydrobenzo[b]thiophen-2-yl)-2-(piperazin-1-yl)acetamide ***(13)*** *[42]*

A solution of intermediate **12** (23.5 mmol) in DCM (95.0 mL) was added in dry RBF and stirred at room temperature, which was followed by the addition of trifluoroacetic acid (TFA) (70.5 mmol). The resulting reaction mixture was stirred at room temperature until completion of the reaction, and reaction progress was monitored on TLC. After completion of the reaction, the mixture was concentrated under a vacuum to yield crude material in gummy form. Crude **13** was purified by washing with diethyl ether (30 mL × 2). After washing **13** was obtained as off-white powder and used in the next step as obtained.

4.2.9. General procedure for synthesis of substituted N-(3-cyano-4,5,6,7-tetrahydrobenzo[b]thiophen-2-yl)-2-(piperazin-1-yl)acetamide ***(14a-o)*** *[39–41]*

To a solution of intermediate **13** (0.75 mmol) with DMF (2.0 mL) in RBF, triethylamine (2.2 mmol) was added, and the reaction mixture was stirred at room temperature for 10 min. Followed by the addition of a solution of commercially available **6a-o** (different substituted aromatic and aliphatic acid chlorides and sulphonyl chlorides) (0.75 mmol) with DMF (1.0 mL) in dropwise manner over the period of 5 min using a glass syringe with maintaining temperature 10 °C. The reaction was moved to room temperature after the complete addition of **6a-o** and progress was monitored on TLC. After completion of the reaction, the temperature was brought to normal temperature, and the reaction mixture was poured into ice-cold water. The precipitates were collected using vacuum filtration and dried. The crude **14a-o** were purified using column chromatography and/or trituration using diethyl ether.

4.2.9.1. N-(3-cyano-4,5,6,7-tetrahydrobenzo[b]thiophen-2-yl)-2-(4-(4-methylbenzoyl)piperazin-1-yl)acetamide ***(14a)***. Compound **14a** was synthesized as per general procedure described above as off white solid in the yield of 70%, mp 144–146 °C. ^{1}H NMR (400 MHz, $CDCl_3$): δ 10.32 (bs, 1H), 7.33–7.31 (d, J = 8, 2H), 7.23–7.21 (d, J = 8, 2H), 3.91 (bs, 1H), 3.60 (bs, 2H), 3.28 (s, 2H), 2.73 (s, 2H), 2.66–2.59 (dt, J = 4, 8, 6H), 2.38 (s, 3H) 1.86–1.81 (m, 3H), 1.67 (s, 2H); ^{13}C NMR (100 MHz, $CDCl_3$): δ 170.5, 166.5, 146.0, 140.1, 132.3, 130.8, 129.1, 128.5, 127.2, 114.2, 94.1, 60.5, 24.09, 24.01, 23.0, 22.0, 21.4. MS (ESI) calcd for $C_{23}H_{26}N_4O_2S$ [M^+] 422.18; found: 423.3 [M+H]. HPLC analysis:

retention time = 7.793 min; peak area = 97.46%; eluent A, ACN; eluent B, H_2O; isocratic (70:30) over 20 min with a flow rate of 1 mL min^{-1}.

4.2.9.2. N-(3-cyano-4,5,6,7-tetrahydrobenzo[b]thiophen-2-yl)-2-(4-(4-methoxybenzoyl) piperazin-1-yl) acetamide ***(14b)***. Compound **14b** was synthesized as per general procedure described above as buff white solid in the yield of 80%, mp 177–179 °C. ^{1}H NMR (400 MHz, $CDCl_3$): δ 10.32 (bs, 1H), 7.41–7.39 (d, J = 8, 2H), 6.93–6.91 (d, J = 8, 2H), 3.84 (s, 3H), 3.66 (bs, 3H), 3.29 (s, 2H), 2.65–2.60 (m, 8H), 1.84–1.83 (d, J = 8, 3H), 1.66 (bs, 2H); ^{13}C NMR (100 MHz, $CDCl_3$): δ 170.3, 166.5, 160.9, 146.0, 130.8, 129.2, 128.5, 127.3, 114.2, 113.7, 94.1, 60.5, 55.3, 53.5, 24.08, 24.01, 23.0, 22.0. MS (ESI) calcd for $C_{23}H_{26}N_4O_3S$ [M^+] 438.17; found: 439.3 [M+H]. HPLC analysis: retention time = 6.693 min; peak area = 100.0%; eluent A, ACN; eluent B, H_2O; isocratic (70:30) over 20 min with a flow rate of 1 mL min^{-1}.

4.2.9.3. 2-(4-Benzoylpiperazin-1-yl)-N-(3-cyano-4,5,6,7-tetrahydrobenzo [b]thiophen-2-yl)acetamide ***(14c)***. Compound **14c** was synthesized as per general procedure described above as white solid in the yield of 72%, mp 192–193 °C. ^{1}H NMR (400 MHz, $CDCl_3$): δ 10.31 (bs, 1H), 7.44–7.70 (m, 5H), 3.93 (bs, 2H), 3.58 (bs, 2H), 3.29 (s, 2H), 2.75 (s, 2H), 2.66–2.59 (dt, J = 4, 8, 6H), 1.87–1.83 (m, 4H); ^{13}C NMR (100 MHz, $CDCl_3$): δ 170.3, 166.5, 146.0, 135.3, 130.8, 129.9, 128.5, 127.0, 126.5, 114.2, 94.1, 60.4, 53.7, 53.2, 47.8, 42.2, 24.07, 24.00, 23.0, 22.0. MS (ESI) calcd for $C_{22}H_{24}N_4O_2S$ [M^+] 408.16; found: 409.3 [M+H]. HPLC analysis: retention time = 6.630 min; peak area = 100.0%; eluent A, ACN; eluent B, H_2O; isocratic (70:30) over 20 min with a flow rate of 1 mL min^{-1}.

4.2.9.4. 2-(4-(4-Chlorobenzoyl)piperazin-1-yl)-N-(3-cyano-4,5,6,7-tetrahydrobenzo[b]thiophen-2-yl)acetamide ***(14d)***. Compound **14d** was synthesized as per general procedure described above as brownish white solid in the yield of 60%, mp 152–154 °C. ^{1}H NMR (400 MHz, $CDCl_3$): δ 10.26 (s, 1H), 8.31–8.29 (d, J = 8, 2H), 7.61–7.59 (d, J = 8, 2H), 3.95 (bs, 2H), 3.53 (bs, 2H), 3.32 (s, 2H), 2.79 (s, 2H), 2.66–2.59 (m, 6H), 1.87–1.80 (m, 4H); ^{13}C NMR (100 MHz, $CDCl_3$): δ 168.0, 166.1, 148.5, 146.0, 141.1, 130.8, 128.7, 128.1, 124.0, 114.3, 94.1, 60.4, 53.5, 53.0, 47.6, 42.2, 24.08, 24.00, 23.0, 22.0. MS (ESI) calcd for $C_{22}H_{23}ClN_4O_2S$ [M^+] 442.12; found: 443.5 [M+H], 445.6 [M+2]. HPLC analysis: retention time = 8.307 min; peak area = 100.0%; eluent A, ACN; eluent B, H_2O; isocratic (70:30) over 20 min with a flow rate of 1 mL min^{-1}.

4.2.9.5. 2-(4-(4-Bromobenzoyl)piperazin-1-yl)-N-(3-cyano-4,5,6,7-tetrahydrobenzo[b]thiophen-2-yl)acetamide ***(14e)***. Compound **14e** was synthesized as per general procedure described above as brownish white solid in the yield of 69%, mp 162–164 °C. ^{1}H NMR (400 MHz, $CDCl_3$): δ 10.68 (s, 1H), 7.58–7.56 (d, J = 8, 2H), 7.32–7.30 (d, J = 8, 2H), 3.98 (bs, 2H), 3.65 (bs, 3H), 0.95 (bs, 2H), 2.63–2.54 (m, 8H), 1.86–1.79 (m, 3H); ^{13}C NMR (100 MHz, $CDCl_3$): δ 169.5, 165.0, 148.5, 145.5, 133.5, 131.9, 131.7, 131.5, 131.1, 128.89, 128.82, 124.6, 114.2, 94.5, 59.3, 52.9, 24.0, 23.9, 23.0, 22.0. MS (ESI) calcd for $C_{22}H_{23}BrN_4O_2S$ [M^+] 486.07; found: 487.3 [M+H], 489.2 [M+2]. HPLC analysis: retention time = 8.353 min; peak area = 96.55%; eluent A, ACN; eluent B, H_2O; isocratic (70:30) over 20 min with a flow rate of 1 mL min^{-1}.

4.2.9.6. Ethyl 2-(4-(2-((3-cyano-4,5,6,7-tetrahydrobenzo[b]thiophen-2-yl)amino)-2-oxoethyl) piperazin-1-yl)-2-oxoacetate ***(14f)***. Compound **14f** was synthesized as per general procedure described above as white solid in the yield of 78%, mp 198–200 °C. ^{1}H NMR (400 MHz, $CDCl_3$): δ 10.23 (s, 1H), 4.37–4.32 (q, J = 4, 12, 2H), 3.79 (bs, 2H), 3.61–3.59 (t, J = 8, 2H), 3.31 (s, 2H), 2.73–2.71 (t, J = 8, 4H), 2.66–2.58 (dt, J = 4, 8, 4H), 1.87–1.81 (m, 4H), 1.39–1.36 (t, J = 12, 3H),; ^{13}C NMR (100 MHz, $CDCl_3$): δ 166.2, 162.3, 160.0, 145.9, 130.8, 128.6, 114.2, 94.2, 62.3, 60.4, 53.2, 52.6, 47.8, 46.0, 41.4, 24.07, 24.00, 23.0, 22.0, 14.0. MS (ESI) calcd for $C_{19}H_{24}N_4O_4S$ [M^+] 404.15; found: 405.3 [M+H]. HPLC analysis: retention time = 5.703 min; peak area = 100.0%; eluent A, ACN; eluent B, H_2O; isocratic (70:30) over 20 min with a flow rate of 1 mL min^{-1}.

4.2.9.7. N-(3-cyano-4,5,6,7-tetrahydrobenzo[b]thiophen-2-yl)-2-(4-(4-nitrobenzoyl)piperazin-1-yl)acetamide ***(14g)***. Compound **14g** was synthesized as per general procedure described above as yellowish solid in the yield of 63%, mp 208–209 °C. ^{1}H NMR (400 MHz, $CDCl_3$): δ 10.27 (s, 1H), 8.31–8.29 (d, J = 8, 2H), 7.61–7.59 (d, J = 8, 2H), 3.95 (s, 2H), 3.53 (bs, 2H), 3.32 (s, 2H), 2.79 (s, 2H), 2.65–2.59 (m, 6H), 1.85–1.82 (m, 4H); **^{13}C NMR** (100 MHz, $CDCl_3$): δ 168.0, 166.1, 148.4, 146.0, 141.4, 130.8, 128.7, 128.1, 124.0, 114.3, 95.6, 94.1, 60.4, 53.5, 53.0, 47.6, 42.2, 24.08, 24.0, 23.0, 22.0. MS (ESI) calcd for $C_{22}H_{23}N_5O_4S$ [M^+] 453.15; found: 454.3 [M+H]. HPLC analysis: retention time = 6.320 min; peak area = 100.0%; eluent A, ACN; eluent B, H_2O; isocratic (70:30) over 20 min with a flow rate of 1 mL min^{-1}.

4.2.9.8. 2-(4-Acetylpiperazin-1-yl)-N-(3-cyano-4,5,6,7-tetrahydrobenzo [b]thiophen-2-yl)acetamide ***(14h)***. Compound **14h** was synthesized as per general procedure described above as white solid in the yield of 94%, mp 146–148 °C. ^{1}H NMR (400 MHz, $CDCl_3$): δ 10.30 (s, 1H), 3.75 (bs, 2H), 3.62–3.59 (t, J = 12, 2H), 3.28 (s, 2H), 3.03–3.00 (t, J = 12, 1H), 2.70–2.61 (m, 7H), 2.12 (s, 3H), 1.88–1.80 (m, 4H); ^{13}C NMR (100 MHz, $CDCl_3$): δ 169.0, 167.3, 166.5, 166.3, 160.7, 146.2, 146.0, 130.87, 130.85, 128.6, 128.5, 128.2, 114.2, 94.19, 94.14, 93.8, 61.0, 60.5, 60.4, 54.3, 53.8, 53.4, 53.1, 52.7, 46.3, 46.1, 45.6, 41.4, 39.9, 24.07, 24.00, 23.0, 22.0, 21.3. MS (ESI) calcd for $C_{17}H_{22}N_4O_2S$ [M^+] 346.15; found: 347.3 [M+H]. HPLC analysis: retention time = 7.52 min; peak area = 98.89%; eluent A, ACN; eluent B, H_2O; isocratic (85:15) over 20 min with a flow rate of 1 mL min^{-1}.

4.2.9.9. N-(3-cyano-4,5,6,7-tetrahydrobenzo[b]thiophen-2-yl)-2-(4-(phenylsulfonyl)piperazin-1-yl)acetamide ***(14i)***. Compound **14i** was synthesized as per general procedure described above as off white solid in the yield of 80%, mp 178–180 °C. ^{1}H NMR (400 MHz, $CDCl_3$): δ 9.90 (s, 1H), 7.71–7.70 (d, J = 4, 2H), 7.60–7.56 (t, J = 8, 1H), 7.50–7.52 (d, J = 8, 2H), 3.17 (bs, 2H), 3.11(bs, 3H), 2.67–2.65 (t, J = 4, 4H), 2.55–2.45 (dt, J = 4, 8, 4H), 1.79–1.69 (m, 4H), 1.60 (s, 1H); ^{13}C NMR (100 MHz, $CDCl_3$): δ 166.2, 145.8, 133.5, 133.2, 130.8, 129.2, 128.6, 127.5, 114.2, 94.1, 60.2, 52.5, 46.1, 24.0, 23.9, 23.0, 22.0. MS (ESI) calcd for $C_{21}H_{24}N_4O_3S_2$[M^+] 444.13; found: 445.4 [M+H]. HPLC analysis: retention time = 7.837 min; peak area = 97.44%; eluent A, ACN; eluent B, H_2O; isocratic (70:30) over 20 min with a flow rate of 1 mL min^{-1}.

4.2.9.10. N-(3-cyano-4,5,6,7-tetrahydrobenzo[b]thiophen-2-yl)-2-(4-tosylpiperazin-1-yl)acetamide ***(14j)***. Compound **14j** was synthesized as per general procedure described above as off white solid in the yield of 76%, mp 230–232 °C. ^{1}H NMR (400 MHz, $CDCl_3$): δ 9.86 (s, 1H), 7.59–7.57 (d, J = 8, 2H), 7.30–7.28 (d, J = 8, 2H), 3.63 (s, 1H), 3.17 (s, 2H), 3.09 (bs, 3H), 2.66–2.64 (t, J = 8, 4H), 2.56–2.48 (dt, J = 4, 8, 4H), 2.38 (s, 3H), 1.75–1.70 (m, 4H); ^{13}C NMR (100 MHz, $CDCl_3$): δ 166.3, 145.7, 144.0, 132.5, 130.8, 129.9, 128.6, 127.6, 114.1, 94.1, 67.0, 60.2, 52.6, 46.0, 24.0, 23.9, 23.0, 22.0, 21.6. MS (ESI) calcd for $C_{22}H_{26}N_4O_3S_2$[M^+] 458.14; found: 459.3 [M+H]. HPLC analysis: retention time = 9.227 min; peak area = 100%; eluent A, ACN; eluent B, H_2O; isocratic (70:30) over 20 min with a flow rate of 1 mL min^{-1}.

4.2.9.11. N-(3-cyano-4,5,6,7-tetrahydrobenzo[b]thiophen-2-yl)-2-(4-((4-methoxyphenyl)sulfonyl) piperazin-1-yl)acetamide ***(14k)***. Compound **14k** was synthesized as per general procedure described above as brownish white solid in the yield of 80%, mp 236–238 °C. ^{1}H NMR (400 MHz, $CDCl_3$): δ 9.88 (s, 1H), 7.64–7.62 (d, J = 8, 2H), 6.97–6.94 (d, J = 12, 2H), 3.82 (s, 3H), 3.17 (s, 2H), 3.08 (bs, 3H), 2.67–2.64 (t, J = 12, 4H), 2.56–2.46 (dt, J = 8, 12, 4H), 1.78–1.70 (m, 5H); ^{13}C NMR (100 MHz, $CDCl_3$): δ 166.38, 166.30, 145.7, 130.8, 129.7, 128.6, 126.9, 114.4,

114.1, 94.1, 60.2, 55.6, 52.6, 46.0, 24.0, 23.9, 23.0, 22.0. MS (ESI) calcd for $C_{22}H_{26}N_4O_4S_2[M^+]$ 474.14; found: 475.4 [M+H]. HPLC analysis: retention time = 8.420 min; peak area = 98.94%; eluent A, ACN; eluent B, H_2O; isocratic (70:30) over 20 min with a flow rate of 1 mL min^{-1}.

4.2.9.12. 2-(4-((4-Chlorophenyl)sulfonyl)piperazin-1-yl)-N-(3-cyano-4,5,6,7-tetrahydrobenzo[b] thiophen-2-yl)acetamide ***(14l)***. Compound **14l** was synthesized as per general procedure described above as off white solid in the yield of 75%, mp 223–225 °C. ^{1}H NMR (400 MHz, $CDCl_3$): δ 9.90 (s, 1H), 7.65–7.63 (d, J = 8, 2H), 7.48–7.46 (d, J = 8, 2H), 3.19 (s, 2H), 3.13 (bs, 3H), 2.68–2.66 (t, J = 8, 4H), 2.56–2.47 (dt, J = 4, 12, 4H), 1.78–1.70 (m, 5H); ^{13}C NMR (100 MHz, $CDCl_3$): δ 166.2, 145.7, 139.8, 134.1, 130.8, 129.6, 129.0, 128.6, 114.2, 94.2, 60.1, 52.5, 46.0, 24.0, 23.9, 23.0, 22.0. MS (ESI) calcd for $C_{21}H_{23}ClN_4O_3S_2[M^+]$ 478.09; found: 479.3 [M+H], 481.3 [M+2]. HPLC analysis: retention time = 10.280 min; peak area = 99.28%; eluent A, ACN; eluent B, H_2O; isocratic (70:30) over 20 min with a flow rate of 1 mL min^{-1}.

4.2.9.13. N-(3-cyano-4,5,6,7-tetrahydrobenzo[b]thiophen-2-yl)-2-(4-(thiophen-2-yl-sulfonyl) piperazin-1-yl)acetamide ***(14m)***. Compound **14m** was synthesized as per general procedure described above as brownish solid in the yield of 60%, mp 195–197 °C. ^{1}H NMR (400 MHz, $CDCl_3$): δ 9.96 (s, 1H), 7.62–7.60 (d, J = 8, 1H), 7.51–7.50 (m, 1H), 7.13–7.11 (t, J = 8, 1H), 3.20 (s, 2H), 3.16 (s, 3H), 2.72–2.69 (t, J = 12, 4H), 2.57–2.47 (dt, J = 4, 12, 4H), 1.78–1.73 (m, 4H), 1.71 (s, 1H); ^{13}C NMR (100 MHz, $CDCl_3$): δ 166.2, 145.8, 135.4, 132.7, 132.6, 130.8, 128.6, 127.8, 114.2, 94.1, 60.1, 52.4, 46.2, 24.0, 23.9, 23.0, 22.0. MS (ESI) calcd for $C_{19}H_{22}N_4O_3S_3[M^+]$ 450.09; found: 451.2 [M+H]. HPLC analysis: retention time = 7.783 min; peak area = 100%; eluent A, ACN; eluent B, H_2O; isocratic (70:30) over 20 min with a flow rate of 1 mL min^{-1}.

4.2.9.14. N-(3-cyano-4,5,6,7-tetrahydrobenzo[b]thiophen-2-yl)-2-(4-(methylsulfonyl)piperazin-1-yl)acetamide ***(14n)***. Compound **14n** was synthesized as per general procedure described above as white solid in the yield of 85%, mp 217–219 °C. ^{1}H NMR (400 MHz, $CDCl_3$): δ 10.27 (s, 1H), 3.64 (s, 1H), 3.32 (s, 3H), 3.25 (s, 2H), 2.77 (s, 3H), 2.74–2.71 (t, J = 12, 4H), 2.59–2.51 (dt, J = 4, 8, 4H), 1.81–1.73 (m, 4H); ^{13}C NMR (100 MHz, $CDCl_3$): δ 166.2, 146.2, 130.7, 128.6, 114.5, 94.0, 67.1, 60.1, 52.6, 46.0, 34.2, 24.09, 24.00, 23.0, 22.0. MS (ESI) calcd for $C_{16}H_{22}N_4O_3S_2[M^+]$ 382.11; found: 383.3 [M+H]. HPLC analysis: retention time = 5.063 min; peak area = 100%; eluent A, ACN; eluent B, H_2O; isocratic (70:30) over 20 min with a flow rate of 1 mL min^{-1}.

4.2.9.15. N-(3-cyano-4,5,6,7-tetrahydrobenzo[b]thiophen-2-yl)-2-(4-((4-fluorophenyl)sulfonyl) piperazin-1-yl)acetamide ***(14o)***. Compound **14o** was synthesized as per general procedure described above as white solid in the yield of 85%, mp 210–212 °C. ^{1}H NMR (400 MHz, $CDCl_3$): δ 9.93 (s, 1H), 7.74–7.69 (m, 2H), 7.21–7.15 (m, 2H), 3.19 (s, 2H), 3.11 (s, 3H), 2.69–2.66 (t, J = 12, 4H), 2.56–2.46 (dt, J = 4, 8, 4H), 2.38 (s, 4H), 1.75–1.70 (m, 1H), 1.60 (s, 1H); ^{13}C NMR (100 MHz, $CDCl_3$): δ 166.7, 166.2, 164.1, 145.8, 131.5, 131.4, 130.8, 130.3, 130.2, 128.6, 116.6, 116.5, 114.1, 94.2, 60.1, 52.5, 46.1, 24.0, 23.9, 23.0, 22.0. MS (ESI) calcd for $C_{21}H_{23}FN_4O_3S_2[M^+]$ 462.12; found: 463.3 [M+H]. HPLC analysis: retention time = 8.447 min; peak area = 98.29%; eluent A, ACN; eluent B, H_2O; isocratic (70:30) over 20 min with a flow rate of 1 mL min^{-1}.

4.2.10. General procedure for the synthesis of 2-(4-(4-aminobenzoyl) piperazin-1-yl)-N-(3-cyano-4,5,6,7-tetrahydrobenzo[b]thiophen-2-yl) acetamide ***(15)*** *[44,45]*

In a clean RBF, **14g** (2.2 mmol) was added in a mixture of methanol (1.0 mL) and water (0.5 mL). To this reaction mixture, dry activated zinc (11 mmol) was added and followed by the addition of NH_4Cl (11 mmol). The resulting mixture was stirred at 45 °C until completion of the reaction. Progress of the reaction was monitored on TLC. After completion of the reaction, the reaction mixture was poured into ice-cold water and extracted with ethyl acetate (10 mL × 2). The combined organic layer was dried over anhydrous Na_2SO_4 and concentrated in vacuo. Crude **15** was purified by column chromatography using hexane: ethyl acetate (60:40) as a mobile phase.

4.2.10.1. 2-(4-(4-Aminobenzoyl)piperazin-1-yl)-N-(3-cyano-4,5,6,7-tetrahydrobenzo[b]thiophen-2-yl)acetamide ***(15)***. Compound **15** was synthesized as per general procedure described above as pale yellowish white solid in the yield of 60%, mp 136–138 °C. ^{1}H NMR (400 MHz, DMSO-d_6): δ 11.21 (bs, 1H), 7.13–7.11 (d, J = 8, 2H), 6.56–6.54 (d, J = 8, 2H), 5.54 (s, 2H), 3.53 (bs, 4H), 2.60–2.55 (m, 5H), 2.49(bs, 5H), 1.75 (bs, 4H); ^{13}C NMR (100 MHz, DMSO-d_6): δ 169.8, 167.7, 150.5, 146.0, 130.5, 129.2, 127.4, 114.1, 112.6, 93.1, 59.5, 52.4, 23.4, 23.3, 22.5, 21.6. MS (ESI) calcd for $C_{22}H_{25}N_5O_2S$ $[M^+]$ 423.17; found: 424.3 [M+H]. HPLC analysis: retention time = 5.10 min; peak area = 100.0%; eluent A, ACN; eluent B, H_2O; isocratic (70:30) over 20 min with a flow rate of 1 mL min^{-1}.

4.3. Biological assay methods

4.3.1. In vitro HeLa cell broth [47]

The HDAC inhibitory activity was determined using a colorimetric-based EpiQuik HDAC activity/inhibition assay kit (Epigentek, Farmingdale, NY). Briefly, HeLa cells were treated with the synthesised compounds (10 μmol) for 24 h. The cell pellets were collected and re-suspended in lysis buffer and incubated under shaking for 30 min at 4 °C to prepare the nuclear fractions. This was centrifuged at 14,000*g* for 10 min at 4 °C, and the supernatants (nuclear fractions) were stored at −80 °C for further tests. Initially, the biotinylated HDAC substrate was added to a 96-well strip plate and incubated for 45 min. HDAC assay buffer and prepared nuclear extracts (2 μL) were added to the plate after washing and incubated for 1 h. Then, the plates were treated with antibody capture and incubated for 1 h. After incubation, antibody detection and developing solution were added. After addition of the stop solution, the absorbance was measured at 450 nm in an ELISA plate reader (Bio-Tek Instruments Inc.). Vorinostat was used as a positive control (Sigma, India). The given formula was used to calculate HDAC inhibition.

% Inhibition = (1 − [(control – blank) – (inhibitor sample – blank)]/[(control – blank) – (no inhibitor sample – blank)] × 100%.

4.3.2. In vitro HDACs isoform selectivity assay

HDACs isoform selectivity inhibition assays were conducted based on the previously reported fluorescent assay system [48]. FLUOR DE LYS® deacetylase substrate based on residues 379–382 of p53 (Arg-His-Lys-Lys(Ac), BML-KI 177, Enzo) was used for HDAC1, 2, and 6 (Signalchem). A synthesized fluorogenic HDAC class II substrate Boc-Lys (TFA)-AMC was used as a substrate for HDAC4 (Signalchem) [49]. HDAC assay buffer (BPS), developer*2 (BPS), and DMSO (nacalai) were also used in the assays. Experiments were conducted in 96-well black plates (Corning Incorporated, 3694) according to the following protocol. Synthesized compounds (5% DMSO in HDAC assay buffer, 10 μL/well) and HDACs solution (1.0 ng/μL in HDAC assay buffer, 20 μL/well) were incubated for 10 min at 25 °C. Then, the reaction was started by the addition of substrate (12.5 μM in HDAC assay buffer, 20 μL/well) and incubated for 3 h at 25 °C. Reaction was stopped by addition developer*2 (doubling dilution with HDAC assay buffer, 50 μL/well) and further incubated for 30 min at 25 °C. The fluorescence was measured by Ensight® readers (PerkinElmer Ltd.) with excitation at 380 nm and emission at 460 nm. The IC_{50} values were calculated from five data point dose response curve (n = 3) and determined by regression analysis of the concentration/inhibition data by GraFit 7.

4.3.3. In vitro antiproliferative assay [50]

In vitro antiproliferative assay was performed using Cell Quanti-MTT cell viability assay kit (Bioassay Systems) using MDA-MB-231, A549, HeLa and hTERT RPE-1 cell lines (2×10^5 cells per well). MDA-MB-231 (human breast cancer), A549 (lung cancer) HeLa (human cervical carcinoma), and hTERT-RPE1 (normal retina epithelial cells immortalized with hTERT) cells were obtained from NCCS (Pune, India) and maintained in medium DMEM and DMEM F12 (Gibco, Bangalore, India) supplemented by 10 percent FBS (V/V), streptomycin (100 g/L) and penicillin (100 IU/mL) (Himedia) to prevent microbial contamination. In 96-well flat bottom titer plate, the MDA-MB-231, A549, HeLa and hTERT RPE-1 cells were seeded at a density of 2×10^5 cells per well and incubated at 37 °C for 24 h in an atmosphere containing 5% CO_2. The media was extracted and replaced by a fresh medium containing synthesized compounds at different concentrations and incubated at 37 °C for 24 h. After incubation, the culture media was drained and washed thrice with phosphate buffer saline (PBS) and incubated at 37 °C for 4 h with 100 μL of MTT (5 mg/mL in PBS). Then the MTT was substituted with 100 μL DMSO and blended well to remove the insoluble formazan. Further, the absorbance was measured at 570 nm using a microplate reader (Lark, India). The percentage of cell viability was calculated using the formula:

Cell viability (%) = (absorbance of sample/absorbance of control) × 100, and further IC_{50} was determined using GraphPad prism 8.0.

4.3.4. Cell death analysis (FACS) and cell cycle analysis

4.3.4.1. Cell lines. U937 and MDA-MB-231cells were purchased from DSMZ and grown following standard protocols at 37 °C with 5% CO_2, in RPMI (U937 cells) and DMEM (MDA-MB-231) supplemented with 10% fetal bovine serum (FBS; Gibco), 2 mM L-glutamine (Euroclone), and antibiotics (100 U/mL penicillin, 100 μg/mL streptomycin, and 250 ng/mL amphotericin-B; Euroclone). Cells were mycoplasma free, tested by EZ-PCR Mycoplasma Test Kit (Biological Industries). Cells were used for experiments between passages 10 to 20 and then discarded.

4.3.4.2. Antibodies. Cyclin A and actin were purchased from Santa Cruz. Acetyl tubulin was purchased from from Sigma. Cyclin D, cyclin E, and histone H4 were purchased from Abcam. GAPDH from Cell Signaling, and histone H3 K9/14ac was purchased from Diagenode.

4.3.5. Cell cycle and cell death analysis [51]

For cell cycle analysis and sub-G1 evaluation, U937 and MDA-MB-231, after stimulation were harvested with PBS, centrifuged, and re-suspended in 500 μL of a hypotonic solution (1X PBS, 0.1% sodium citrate, 0.1% NP-40, RNAase A, and 50 mg/mL PI). For cell death evaluation, cells were harvested with PBS, centrifuged at 1200 rpm for 5 min, and re-suspended in 500 μL 1X PBS and 0.2 mg/mL PI. Data was acquired using the BD Accuri TM C6 flow cytometer system (BD Biosciences). Each experiment was performed in biological triplicates and values expressed as mean ± SD.

4.3.6. Western blot analysis

After treatment, cells were washed and lysed in two specific buffers, one for protein total extract and one for histone proteins extract. For total protein extract, lysis reaction was carried out for 15 min at 4 °C in a specific buffer (50 mM Tris-HCl pH 7.4, 150 mM NaCl, 1% NP-40, 10 mM NaF, 1 mM PMSF and protease inhibitors). Histone proteins were obtained as suspended cellular pellet into triton extraction buffer (TEB) (PBS containing 0.5% Triton X 100 (v/v), 2 mM PMSF, 0.02% (w/v) NaN_3). The lysis was performed for 10 min at 4 °C. After centrifugation pellets were washed in TEB (half volume) and then resuspended in 0.2 N HCl. Acid histone extraction was carried out overnight at 4 °C. Proteins concentration was quantified by Bradford assay (Bio-Rad).

Western blot was performed by lodging 50 μg total extract into 10–15% polyacrylamide gels and 5 μg of histone extract into 15%, and then transferred to a nitrocellulose membrane using a transfer apparatus according to the manufacturer's protocols (Bio-Rad). After blocking step in 5% non-fat milk in TBST (10 mM Tris pH 8.0, 150 mM NaCl, 0.5% TWEEN 20) for 60 min, the membrane was washed in TBST and incubated with antibodies. Detection was performed with an ECL system (Amersham Biosciences) according to the manufacturer's protocol.

4.3.7. In vitro microsomal stability

A 10 mM stock solution of **9h**, **14n** and verapamil was prepared in DMSO. From the intermediate stock solution of 2 mM, a working solution of 0.5 mM was prepared by diluting the compounds in acetonitrile: water (50:50). The compounds (1.8 μL of working solution) were spiked in 0.1 M potassium phosphate buffer (260.7 μL) at pH 7.4 and a concentration of 3 μM (0.1% DMSO). Following this, human and rat liver microsomes (Invitrogen) (7.5 μL, final protein concentration was 0.5 mg/mL) were added. The aforementioned sample was incubated at 37 °C for 5 min. Subsequently, 30 μL of 10 mM NADPH prepared in 0.1 M potassium phosphate buffer was added (as a co-factor) to initiate the reaction. The samples were then incubated at 37 °C for desired time points.

At each time point (0, 5, 15, 30, 60, and 120 min), 40 μL of the samples were withdrawn and reactions were stopped using 360 μL chilled acetonitrile or methanol containing suitable internal standard (carbamazepine). The samples were centrifuged and the supernatants were analyzed in duplicate by LC-MS/MS. The percent compound remaining at each time point was calculated with respect to that of the 0 min sample. The data were then analyzed in duplicate to calculate half-life and intrinsic clearance (CLint). Control samples were run without NADPH for initial and final time point and blank samples were prepared using DMSO (without the test compounds).

4.4. In silico ADME evaluation

Pharmacokinetic and physicochemical properties such partition coefficient (log $P_{o/w}$), aqueous solubility (log S), molecular weight (MW), hydrogen bod donor (HBD), hydrogen bond acceptor (HBA), total polar surface area (TPSA), molar refractivity (MR), number of rotatable bonds with passive gastrointestinal absorption (GIA), brain penetration (BBB) and cytochromes P_{450} (CYPs) inhibition were predicted for the synthesized compounds of both the series and comapared with vorinostat using online workstation SwissADME [52]. SwissADME is freely available at http://www.swissadme.ch/index.php#.

4.5. Molecular docking

Docking study was performed using Gold 5.2.2 software on Intel Chipset with Intel Core i3 second generation processor, 4 GB DDR3 RAM, and a clock speed of 3.3 GHZ [17]. We docked synthesized compounds in HDAC6 protein (PDB ID: 5G0G, 1.499 Å) co-crystallized with trichostatin A. HDAC6 co-crystallized structure was downloaded and imported in the GOLD wizard. Hydrogen atoms were added and water molecules were deleted. Crystallized trichostatin A was extracted and a docking site was created. Synthesized compounds were imported with reference standard ligand. The gold score was used as a fitness function to evaluate the score of compounds.

Author contributions

The P.G. and M.D.G. designed the study. P.G. synthesized all the molecules. P.G., and N.S. characterized all the synthesized molecules. P. G. and V.K.V. designed and performed all the computational studies. V. R. and K.S. performed a HeLa broth inhibition assay. V.C., L.D.T., A.P performed cell cycle analysis, cell death evaluation, and western blot analysis. L.A. evaluated the biomedical analyses and anticancer data. T. K., and T.S, performed an HDAC enzyme inhibition assay. D.G., and D.B

performed an MTT assay. V.S. performed *in vitro* microsomal stability assay. The manuscript was written by P.G., V.K.V., M.D.G., and also through the contributions of all the co-authors. All co-authors have approved the final version of this manuscript.

Declaration of Competing Interest

The authors declare that they have no known competing financial interests or personal relationships that could have appeared to influence the work reported in this paper.

Acknowledgment

All of the authors are grateful to DST INSPIRE-Department of Science and Technology, INDIA for financial assistance under Project number DST INSPIRE/IF160300. Vanvitelli per la Ricerca: "CAMPANIA" (ID 342) and "AdipCare" (ID 263); Campania Regional Government Technology Platform Lotta alle Patologie Oncologiche: iCURE (B21C17000030007); Campania Regional Government FASE2: IDEAL (B63D18000560007). MIUR, Proof of Concept POC01_00043; AP holds a PhD fellowship coded 'B25D18000010006' PON-2017; LDT holds a PhD fellowship coded 'B27D18001030006' PON-2018. PG is thankful to all the collaborators for their kind support in this research. This research work is a part of the Ph.D. thesis of Piyush Gediya (PG), Institute of Pharmacy, Nirma University, Ahmedabad, India.

Appendix A. Supplementary material

Supplementary data to this article can be found online at https://doi.org/10.1016/j.bioorg.2021.104801.

References

[1] P.A. Marks, R.A. Rifkind, V.M. Richon, R. Breslow, T. Miller, W.K. Kelly, Histone deacetylases and cancer: causes and therapies, Nat. Rev. Cancer. 1 (3) (2001) 194–202.
[2] T.C.S. Ho, A.H.Y. Chan, A. Ganesan, Thirty Years of HDAC Inhibitors: 2020 Insight and Hindsight, J. Med. Chem. (2020).
[3] A. Nebbioso, V. Carafa, R. Benedetti, L. Altucci, Trials with "epigenetic" drugs: an update, Mol. Oncol. 6 (2012) 657–682.
[4] A. Nebbioso, V. Carafa, M. Conte, F.P. Tambaro, C. Abbondanza, J. Martens, M. Nees, R. Benedetti, I. Pallavicini, S. Minucci, G. Garcia-Manero, F. Iovino, G. Lania, C. Ingenito, V. Belsito Petrizzi, H.G. Stunnenberg, L. Altucci, c-Myc modulation and acetylation is a key HDAC inhibitor target in cancer, Clin. Cancer Res. an Off. J. Am. Assoc. Cancer Res. 23 (10) (2017) 2542–2555.
[5] G.P. Delcuve, D.H. Khan, J.R. Davie, Roles of histone deacetylases in epigenetic regulation: emerging paradigms from studies with inhibitors, Clin. Epigenet. 4 (2012) 5.
[6] L. Whitehead, M.R. Dobler, B. Radetich, Y. Zhu, P.W. Atadja, T. Claiborne, J. E. Grob, A. McRiner, M.R. Pancost, A. Patnaik, W. Shao, M. Shultz, R. Tichkule, R. A. Tommasi, B. Vash, P. Wang, T. Stams, Human HDAC isoform selectivity achieved via exploitation of the acetate release channel with structurally unique small molecule inhibitors, Bioorg. Med. Chem. 19 (15) (2011) 4626–4634.
[7] F. He, Y. Ran, X. Li, D. Wang, Q. Zhang, J. Lv, C. Yu, Y. Qu, X. Zhang, A. Xu, C. Wei, C.J. Chou, J. Wu, Design, synthesis and biological evaluation of dual-function inhibitors targeting NMDAR and HDAC for Alzheimer's disease, Bioorg. Chem. 103 (2020), 104109.
[8] M.F.A. Mohamed, B.G.M. Youssif, M.S.A. Shaykoon, M.H. Abdelrahman, B.E. M. Elsadek, A.S. Aboraia, G.-E.-D.-A. Abuo-Rahma, Utilization of tetrahydrobenzo [4,5]thieno[2,3-d]pyrimidinone as a cap moiety in design of novel histone deacetylase inhibitors, Bioorg. Chem. 91 (2019), 103127.
[9] X. Li, Y.K. Peterson, E.S. Inks, R.A. Himes, J. Li, Y. Zhang, X. Kong, C.J. Chou, Class I HDAC inhibitors display different antitumor mechanism in leukemia and prostatic cancer cells depending on their p53 status, J. Med. Chem. 61 (6) (2018) 2589–2603.
[10] M. Duvic, R. Talpur, X. Ni, C. Zhang, P. Hazarika, C. Kelly, J.H. Chiao, J.F. Reilly, J. L. Ricker, V.M. Richon, S.R. Frankel, Phase 2 trial of oral vorinostat (suberoylanilide hydroxamic acid, SAHA) for refractory cutaneous T-cell lymphoma (CTCL), Blood 109 (2007) 31–39.
[11] P. Atadja, Development of the pan-DAC inhibitor panobinostat (LBH589): successes and challenges, Cancer Lett. 280 (2) (2009) 233–241.
[12] O.A. O'Connor, S. Horwitz, T. Masszi, A. Van Hoof, P. Brown, J. Doorduijn, G. Hess, W. Jurczak, P. Knoblauch, S. Chawla, G. Bhat, M.R. Choi, J. Walewski, K. Savage, F. Foss, L.F. Allen, A. Shustov, Belinostat in patients with relapsed or refractory peripheral T-cell lymphoma: results of the pivotal phase II BELIEF (CLN-19) study, J. Clin. Oncol. 33 (2015) 2492–2499.
[13] A.P. Zorzi, M. Bernstein, Y. Samson, D.A. Wall, S. Desai, D. Nicksy, N. Wainman, E. Eisenhauer, S. Baruchel, A phase I study of histone deacetylase inhibitor, pracinostat (SB939), in pediatric patients with refractory solid tumors: IND203 a trial of the NCIC IND program/C17 pediatric phase I consortium, Pediatr. Blood Cancer 60 (2013) 1868–1874.
[14] L. Gore, M.L. Rothenberg, C.L. O'Bryant, M.K. Schultz, A.B. Sandler, D. Coffin, C. McCoy, A. Schott, C. Scholz, S.G. Eckhardt, A Phase I and pharmacokinetic study of the oral histone deacetylase inhibitor, MS-275, in patients with refractory solid tumors and lymphomas, Clin. Cancer Res. 14 (14) (2008) 4517–4525.
[15] S.J. Haggarty, K.M. Koeller, J.C. Wong, R.A. Butcher, S.L. Schreiber, Multidimensional chemical genetic analysis of diversity-oriented synthesis-derived deacetylase inhibitors using cell-based assays, Chem. Biol. 10 (5) (2003) 383–396.
[16] V.K. Vyas, B. Variya, M.D. Ghate, Design, synthesis and pharmacological evaluation of novel substituted quinoline-2-carboxamide derivatives as human dihydroorotate dehydrogenase (hDHODH) inhibitors and anticancer agents, Eur. J. Med. Chem. 82 (2014) 385–393.
[17] N.D. Sitwala, V.K. Vyas, B.C. Variya, S.S. Patel, C.C. Mehta, D.N. Rana, M.D. Ghate, Liquid phase combinatorial synthesis of 1,2,5-trisubstituted benzimidazole derivatives as human DHODH inhibitors, Bioorg. Chem. 75 (2017) 118–126.
[18] P.K. Parikh, M.D. Ghate, Recent advances in the discovery of small molecule c-Met Kinase inhibitors, Eur. J. Med. Chem. 143 (2018) 1103–1138.
[19] T.A. Miller, D.J. Witter, S. Belvedere, Histone deacetylase inhibitors, J. Med. Chem. 46 (24) (2003) 5097–5116.
[20] M.M. Abdel-Atty, N.A. Farag, S.E. Kassab, R.A.T. Serya, K.A.M. Abouzid, Design, synthesis, 3D pharmacophore, QSAR, and docking studies of carboxylic acid derivatives as Histone Deacetylase inhibitors and cytotoxic agents, Bioorg. Chem. 57 (2014) 65–82.
[21] K.J. Coe, T. Koudriakova, Metabolic stability assessed by liver microsomes and hepatocytes, in: Optim. Drug Discov., Springer, 2014, pp. 87–99.
[22] G.W. Caldwell, Z. Yan, Optimization in Drug Discovery, Springer, 2016.
[23] A. Lu, H. Luo, M. Shi, G. Wu, Y. Yuan, J. Liu, F. Tang, Design, synthesis and docking studies on benzamide derivatives as histone deacetylase inhibitors, Bioorg. Med. Chem. Lett. 21 (16) (2011) 4924–4927.
[24] H.-Y. Hsieh, H.-C. Chuang, F.-H. Shen, K. Detroja, L.-W. Hsin, C.-S. Chen, Targeting breast cancer stem cells by novel HDAC3-selective inhibitors, Eur. J. Med. Chem. 140 (2017) 42–51.
[25] C. Cheng, F. Yun, J. He, S. Ullah, Q. Yuan, Design, synthesis and biological evaluation of novel thioquinazolinone-based 2-aminobenzamide derivatives as potent histone deacetylase (HDAC) inhibitors, Eur. J. Med. Chem. 173 (2019) 185–202.
[26] T. Abdizadeh, M.R. Kalani, K. Abnous, Z. Tayarani-Najaran, B.Z. Khashyarmanesh, R. Abdizadeh, R. Ghodsi, F. Hadizadeh, Design, synthesis and biological evaluation of novel coumarin-based benzamides as potent histone deacetylase inhibitors and anticancer agents, Eur. J. Med. Chem. 132 (2017) 42–62.
[27] C.M. Marson, C.J. Matthews, S.J. Atkinson, N. Lamadema, N.S.B. Thomas, Potent and selective inhibitors of histone deacetylase-3 containing chiral oxazoline capping groups and a N-(2-Aminophenyl)-benzamide binding unit, J. Med. Chem. 58 (17) (2015) 6803–6818.
[28] S. Gao, J. Zang, Q. Gao, X. Liang, Q. Ding, X. Li, W. Xu, C.J. Chou, Y. Zhang, Design, synthesis and anti-tumor activity study of novel histone deacetylase inhibitors containing isatin-based caps and o-phenylenediamine-based zinc binding groups, Bioorg. Med. Chem. 25 (12) (2017) 2981–2994.
[29] J.C. Bressi, A.J. Jennings, R. Skene, Y. Wu, R. Melkus, R. De Jong, S. O'Connell, C. E. Grimshaw, M. Navre, A.R. Gangloff, Exploration of the HDAC2 foot pocket: Synthesis and SAR of substituted N-(2-aminophenyl)benzamides, Bioorg. Med. Chem. Lett. 20 (2010) 3142–3145.
[30] K. Gewald, Angew. Chem. 73 (1961) 114.
[31] K. Gewald, Chem. Ber. 98 (1965) 3517.
[32] T. Wang, X.-G. Huang, J. Liu, B.o. Li, J.-J. Wu, K.-X. Chen, W.-L. Zhu, X.-Y. Xu, B.-B. Zeng, An efficient one-pot synthesis of substituted 2-aminothiophenes via three-component gewald reaction catalyzed by l -proline, Synlett. (2010) 1351–1354.
[33] X.-G. Huang, J. Liu, J. Ren, T. Wang, W. Chen, B.-B. Zeng, A facile and practical one-pot synthesis of multisubstituted 2-aminothiophenes via imidazole-catalyzed Gewald reaction, Tetrahedron. 67 (34) (2011) 6202–6205.
[34] M. Treu, T. Karner, R. Kousek, H. Berger, M. Mayer, D.B. McConnell, A. Stadler, Microwave-assisted parallel synthesis of fused heterocycles in a novel parallel multimode reactor, J. Comb. Chem. 10 (6) (2008) 863–868.
[35] K. Wang, D. Kim, A. Dömling, Cyanoacetamide MCR (III): Three-component Gewald reactions revisited, J. Comb. Chem. 12 (2010) 111–118.
[36] M. Adib, H. JanatianGhazvini, M. Soheilizad, S. Saeedi, M. Tajbakhsh, M. Amanlou, One-pot four-component synthesis of thieno[2,3-d]pyrimidin-4-amines via sequential Gewald/cyclocondensation reactions, Helv. Chim. Acta 98 (8) (2015) 1079–1086.
[37] M. Feroci, I. Chiarotto, L. Rossi, A. Inesi, Activation of elemental sulfur by electrogenerated cyanomethyl anion: synthesis of substituted 2-aminothiophenes by the Gewald reaction, Adv. Synth. Catal. 350 (2008) 2740–2746.
[38] R.M. Mohareb, W.W. Wardakhan, F.I. Hamed, Synthesis and cytotoxicity of fused thiophene and pyrazole derivatives derived from 2-N-acetyl-3-cyano-4,5,6,7-tetrahydrobenzo[b]thiophene, Med. Chem. Res. 24 (5) (2015) 2043–2054.
[39] T.W. Bousfield, K.P.R. Pearce, S.B. Nyamini, A. Angelis-Dimakis, J.E. Camp, Synthesis of amides from acid chlorides and amines in the bio-based solvent Cyrene™, Green Chem. 21 (13) (2019) 3675–3681.
[40] N. Gernigon, R.M. Al-Zoubi, D.G. Hall, Direct amidation of carboxylic acids catalyzed by ortho-iodo arylboronic acids: catalyst optimization, scope, and preliminary mechanistic study supporting a peculiar halogen acceleration effect, J. Org. Chem. 77 (2012) 8386–8400.

[41] L.i. Zhang, X.-J. Wang, J. Wang, N. Grinberg, D. Krishnamurthy, C.H. Senanayake, An improved method of amide synthesis using acyl chlorides, Tetrahedron Lett. 50 (24) (2009) 2964–2966.
[42] N. Srinivasan, A. Yurek-George, A. Ganesan, Rapid deprotection of N-Boc amines by TFA combined with freebase generation using basic ion-exchange resins, Mol. Divers. 9 (4) (2005) 291–293.
[43] J. Bariwal, E. Van der Eycken, C-N bond forming cross-coupling reactions: an overview, Chem. Soc. Rev. 42 (24) (2013) 9283, https://doi.org/10.1039/c3cs60228a.
[44] S.M. Kelly, B.H. Lipshutz, Chemoselective reductions of nitroaromatics in water at room temperature, Org. Lett. 16 (1) (2014) 98–101.
[45] M. Orlandi, D. Brenna, R. Harms, S. Jost, M. Benaglia, Recent developments in the reduction of aromatic and aliphatic nitro compounds to amines, Org. Process Res. Dev. 22 (4) (2018) 430–445.
[46] Y.M. Albkuri, A.B. RanguMagar, A. Brandt, H.A. Wayland, B.P. Chhetri, C. M. Parnell, P. Szwedo, A. Parameswaran-Thankam, A. Ghosh, C-N cross-coupling reactions of amines with aryl halides using amide-based pincer nickel(II) catalyst, Catal. Lett. 150 (6) (2020) 1669–1678.
[47] R.B. Santos, A.S. Pires, R. Abranches, Addition of a histone deacetylase inhibitor increases recombinant protein expression in Medicago truncatula cell cultures, Sci. Rep. 7 (2017) 16756.
[48] D. Wegener, F. Wirsching, D. Riester, A. Schwienhorst, A fluorogenic histone deacetylase assay well suited for high-throughput activity screening, Chem. Biol. 10 (1) (2003) 61–68.
[49] D. Riester, C. Hildmann, S. Grünewald, T. Beckers, A. Schwienhorst, Factors affecting the substrate specificity of histone deacetylases, Biochem. Biophys. Res. Commun. 357 (2) (2007) 439–445.
[50] T. Kalaivani, C. Rajasekaran, K. Suthindhiran, L. Mathew, Free radical scavenging, cytotoxic and hemolytic activities from Leaves of Acacia nilotica (L.) Wild. ex. Delile subsp. indica (Benth.) Brenan., Evid. Based. Complement. Alternat. Med. 2011 (2011) 274741.
[51] A. Nebbioso, N. Clarke, E. Voltz, E. Germain, C. Ambrosino, P. Bontempo, R. Alvarez, E.M. Schiavone, F. Ferrara, F. Bresciani, A. Weisz, A.R. de Lera, H. Gronemeyer, L. Altucci, Tumor-selective action of HDAC inhibitors involves TRAIL induction in acute myeloid leukemia cells, Nat. Med. 11 (1) (2005) 77–84.
[52] A. Daina, O. Michielin, V. Zoete, SwissADME: a free web tool to evaluate pharmacokinetics, drug-likeness and medicinal chemistry friendliness of small molecules, Sci. Rep. 7 (2017) 42717.